REPORT DOCUMENTATION PAGE

Form Approved OMB NO. 0704-0188

1. REPORT DATE (DD-MM-YYYY)	2. REPORT TYPE	3. DATES COVERED (From - To)
05-02-2019	Final Report	1-Aug-2014 - 31-Jul-2018

4. TITLE AND SUBTITLE
Final Report: Developing regulatory biochemical reaction circuits

5a. CONTRACT NUMBER
W911NF-14-1-0434

5b. GRANT NUMBER

5c. PROGRAM ELEMENT NUMBER
611102

6. AUTHORS

5d. PROJECT NUMBER

5e. TASK NUMBER

5f. WORK UNIT NUMBER

7. PERFORMING ORGANIZATION NAMES AND ADDRESSES

Rutgers, The State University of New Jersey
311 North 5th Street
Armitage Hall, 3rd Floor
Camden, NJ 08102 -1405

8. PERFORMING ORGANIZATION REPORT NUMBER

9. SPONSORING/MONITORING AGENCY NAME(S) AND ADDRESS (ES)

U.S. Army Research Office
P.O. Box 12211
Research Triangle Park, NC 27709-2211

10. SPONSOR/MONITOR'S ACRONYM(S)
ARO

11. SPONSOR/MONITOR'S REPORT NUMBER(S)
65330-LS-YIP.16

12. DISTRIBUTION AVAILIBILITY STATEMENT

Approved for public release; distribution is unlimited.

13. SUPPLEMENTARY NOTES

The views, opinions and/or findings contained in this report are those of the author(s) and should not contrued as an official Department of the Army position, policy or decision, unless so designated by other documentation.

14. ABSTRACT

15. SUBJECT TERMS

16. SECURITY CLASSIFICATION OF:			17. LIMITATION OF ABSTRACT	15. NUMBER OF PAGES	19a. NAME OF RESPONSIBLE PERSON
a. REPORT	b. ABSTRACT	c. THIS PAGE			Jinglin Fu
UU	UU	UU	UU		19b. TELEPHONE NUMBER 856-225-6612

RPPR Final Report
as of 08-Feb-2019

Agency Code:

Proposal Number: 65330LSYIP **Agreement Number: W911NF-14-1-0434**
INVESTIGATOR(S):

Name: Jinglin Fu
Email: jinglin.fu@rutgers.edu
Phone Number: 8562256612
Principal: Y

Organization: **Rutgers, The State University of New Jersey - Camden**
Address: 311 North 5th Street, Camden, NJ 081021405
Country: USA
DUNS Number: 625216556 EIN: 226001086
Report Date: 31-Oct-2018 Date Received: 05-Feb-2019
Final Report for Period Beginning 01-Aug-2014 and Ending 31-Jul-2018
Title: Developing regulatory biochemical reaction circuits
Begin Performance Period: 01-Aug-2014 **End Performance Period:** 31-Jul-2018
Report Term: 0-Other
Submitted By: Jinglin Fu Email: jinglin.fu@rutgers.edu
Phone: (856) 225-6612
Distribution Statement: 1-Approved for public release; distribution is unlimited.

STEM Degrees: 11 **STEM Participants:** 15

Major Goals: Statement of objectives: The proposed research will apply the organizational power of DNA nanotechnology to the challenges of engineering biochemical reaction circuits with regulatory and feedback functions. The specific aims are: (1) Design and construct aptamer lock-controlled DNA nanotweezers that switch conformations upon binding to target pathway molecules. (2) Use designed DNA nanotweezers to assemble multienzyme pathways that can be regulated through feedback of product generation or substrate consumption. (3) Develop logic-gated “swinging arms” to channel the transfer of intermediates in multienzyme pathways for controlling pathway activity and specificity in response to molecular inputs. (4) Construct an artificial electron-transport chain to facilitate electron transfer along a redox potential gradient within the reaction pathway.

Methods to be employed: DNA nanostructures with specific geometries will be designed and used as the assembly platforms for integrating regulatory circuits, nanomechanical properties and multienzyme pathways. In order to modulate reaction kinetics, two regulatory mechanisms of aptamer-based molecular locks and logic-gated swinging arms will be designed to regulate the spatial interactions between catalytic components for activating or inhibiting the specific enzyme pathway activity. Structural characterization and enzyme activity measurements will be employed to determine the critical parameters for assembling functional reaction pathways with high yield.

Technical Aims
AIM 1: Design and construct aptamer lock-controlled DNA nanostructures. We will use aptamers to construct molecular locks that are able to switch conformations upon binding to target small molecules including enzyme cofactors and metal ions. The aptamer locks will be implemented into DNA nanotweezers to regulate the spatial distance between arms. This aim will lay the structural and chemical foundations for feedback regulation.
AIM 1-1. Select and characterize aptamers that bind to enzyme cofactors and metal ions.
AIM 1-2. Design and construct aptamer-based molecular locks that will switch conformations upon binding to target molecules.
AIM 1-3. Integrate the aptamer locks into DNA tweezers to regulate the spatial distance between arms.
AIM 2: Engineer feedback-regulated enzyme systems. We will apply the aptamer-switchable DNA nanostructures to the assembly and regulation of enzyme/cofactor pairs and enzyme pathways. Aptamer locks will sense the presence of cofactors and the external effectors and thereby induce a conformation change in the DNA structures to regulate the distance between enzyme and cofactor, or enzyme pairs. The switchable spatial interaction will activate or inhibit the function of the enzyme systems, which will realize the feedback regulation of enzyme activities in response to the level of reaction substrates, products or effectors.
AIM 2-1. Assemble enzyme and cofactors onto DNA structures and evaluate the spatial parameters that govern activity.

AIM 2-2. Engineer feedback-regulated enzyme reactions in response to external effectors, and cofactors that are consumed (substrates) or generated (products) by the reaction.
AIM 2-3. Feedback regulation of a multienzyme pathway in response to both the reaction intermediates and final products.
AIM 3: Develop logic-gated multienzyme pathway circuits. We will design and engineer swinging arms to channel intermediate in multienzyme pathways. A logic-gated circuit will be incorporated to control the release and activation of swinging arms. In this way, the pathway activity and specificity will be regulated by input DNA strands that trigger the activation of the logic-gated system.
AIM 3-1. Design and construct swinging arm-channeled enzyme pathways.
AIM 3-2. Engineer logic-gated swinging arms.
AIM 3-3. Design and construct logic-gated control of pathway activities and specificities.
AIM 3-4. Develop a tandem logic gate circuit to control a four-enzyme pathway.
AIM 4: Design and construct an artificial electron-transport chain. We will use DNA nanostructures to organize redox cofactors to construct a redox potential gradient. This will guide the electrons from low redox potential to high redox potential within a reaction pathway.
AIM 4-1. Bioconjugation of redox cofactors to DNA molecules.
AIM 4-2. Assemble redox cofactors onto DNA structures and evaluate the spatial parameters that govern electron transfer efficiency.
AIM 4-3. Optimize the geometric arrangements for more efficient and stable electron transfer.

Split AIMS Between YIP and PECASE: The three-year YIP project will demonstrate the proof of concept for aptamer lock-controlled DNA nanostructures that sense NAD and ATP (Aim 1) and feedback-regulated enzyme reactions (Aims 2-1 and 2-2). The PECASE project will extend Aim 1 and 2 to explore additional feedback mechanisms (Aim 2-3), as well as completing Aims 3 and 4 to develop logic-gated multienzyme pathways and the artificial electron-transport chain.

Accomplishments: See attachment

Training Opportunities: We participated High-School Apprenticeship Program (HSAP), Undergraduate Research Apprenticeship Program (URAP) and Research & Engineering Apprenticeship Program (REAP) that were sponsored by Army Education Outreach Program. In addition, we also accepted students from NSF Research Experiences for Undergraduates (REU).

Through these programs, highs school students and undergraduates were able to participate summer research in our lab that was relevant to the YIP project.

1. Total number of undergraduate bachelor degrees awarded: 8
Adriana Pereira, Brett Vaccaro, Gina Disalvo, Gabriele Stankeviciute, Scott Huston, Robert Maloney, John Collins, Sung Won Oh
2. Total number of Master's degree awarded: 3
John Collins, Nouf Alzhrani, Samirah Ghalib
3. Other graduate students: 2
Ariel Lane, Tianran Li
4. Total number of high school students sponsored for summer research: 5
Chae Lee, Olivia Zapfe, Tristan Meier, Elizabeth Bolarinwa, Grace Kresge
5. Total Number of NSF REU students: 2
Karen Gu, Angela Sun

RPPR Final Report
as of 08-Feb-2019

Results Dissemination: 1. 6/27/2018: Rutgers University–Camden Professor Gives South Jersey High School Students Research Experience through the Army Educational Outreach Program
https://news.camden.rutgers.edu/2018/06/rutgers-university-camden-professor-gives-south-jersey-high-school-students-research-experience-through-the-army-educational-outreach-program/
2. 7/26/2017: Army Education Outreach Program Provides Research Experience in Labs for Undergraduates and High School Students.
https://news.camden.rutgers.edu/2017/07/army-education-outreach-program-provides-research-experience-in-labs-for-undergraduates-and-high-school-students/
3. 7/23/2015: Army Education Outreach Program Supports Two Summer Research Projects
https://news.camden.rutgers.edu/2015/07/army-education-outreach-program-supports-two-summer-research-projects/
4. 2/22/2015: Army Education Outreach Program Supports Research Projects for High School and Undergraduate Students at Rutgers University–Camden
https://news.rutgers.edu/news/army-education-outreach-program-supports-research-projects-high-school-and-undergraduate-students/20150211#.XFn9glxKhPZ

Honors and Awards: •Certificate of a mentorship, Army Education Outreach Program (AEOP), 2018
- Cottrell College Science Award, 2015
- Certificate of a Research Mentorship, Rutgers-Camden, 2015-2018
- Proclamation, Board of Chosen Freeholders of the County of the Camden, 2015
- Army Research Office Young Investigator award, 2014

Protocol Activity Status:

Technology Transfer: 1. Jinglin Fu, Sung Won Oh and Adriana Pereira “DNA Logic-gated Proximity Assembly Circuit for Biochemical Sensing” U.S. Patent Application No. 62/647,014.
2. Jinglin Fu, John Collins and Ting Zhang “DNA-crowded Enzyme Complex with Controlled Spatial Confinements” US Provisional Patent. App. No. 62/482,882.

PARTICIPANTS:

Participant Type: PD/PI
Participant: Jinglin Fu
Person Months Worked: 1.00 **Funding Support:**
Project Contribution:
International Collaboration:
International Travel:
National Academy Member: Y
Other Collaborators:

Participant Type: Graduate Student (research assistant)
Participant: John Collins
Person Months Worked: 1.00 **Funding Support:**
Project Contribution:
International Collaboration:
International Travel:
National Academy Member: N
Other Collaborators:

Participant Type: Graduate Student (research assistant)
Participant: Sung Won Oh
Person Months Worked: 2.00 **Funding Support:**
Project Contribution:
International Collaboration:
International Travel:
National Academy Member: N

Other Collaborators:

Participant Type: Research Experience for Undergraduates (REU) Participant
Participant: Angela Sun
Person Months Worked: 2.00 **Funding Support:**
Project Contribution:
International Collaboration:
International Travel:
National Academy Member: N
Other Collaborators:

Participant Type: Research Experience for Undergraduates (REU) Participant
Participant: Karen Gu
Person Months Worked: 2.00 **Funding Support:**
Project Contribution:
International Collaboration:
International Travel:
National Academy Member: N
Other Collaborators:

Participant Type: Undergraduate Student
Participant: Adriana Pereira
Person Months Worked: 2.00 **Funding Support:**
Project Contribution:
International Collaboration:
International Travel:
National Academy Member: N
Other Collaborators:

Participant Type: Undergraduate Student
Participant: Brett Vaccaro
Person Months Worked: 2.00 **Funding Support:**
Project Contribution:
International Collaboration:
International Travel:
National Academy Member: N
Other Collaborators:

Participant Type: Undergraduate Student
Participant: Gabriele Stankeviciute
Person Months Worked: 2.00 **Funding Support:**
Project Contribution:
International Collaboration:
International Travel:
National Academy Member: N
Other Collaborators:

Participant Type: Graduate Student (research assistant)
Participant: Ariel Lane
Person Months Worked: 4.00 **Funding Support:**
Project Contribution:
International Collaboration:
International Travel:

National Academy Member: N
Other Collaborators:

Participant Type: Graduate Student (research assistant)
Participant: Tianran Li
Person Months Worked: 1.00 **Funding Support:**
Project Contribution:
International Collaboration:
International Travel:
National Academy Member: N
Other Collaborators:

Participant Type: Undergraduate Student
Participant: Scott Huston
Person Months Worked: 2.00 **Funding Support:**
Project Contribution:
International Collaboration:
International Travel:
National Academy Member: N
Other Collaborators:

Participant Type: Undergraduate Student
Participant: Robert Maloney
Person Months Worked: 2.00 **Funding Support:**
Project Contribution:
International Collaboration:
International Travel:
National Academy Member: N
Other Collaborators:

Participant Type: High School Student
Participant: Chae Lee
Person Months Worked: 2.00 **Funding Support:**
Project Contribution:
International Collaboration:
International Travel:
National Academy Member: N
Other Collaborators:

Participant Type: High School Student
Participant: Grace Kresge
Person Months Worked: 2.00 **Funding Support:**
Project Contribution:
International Collaboration:
International Travel:
National Academy Member: N
Other Collaborators:

Participant Type: High School Student
Participant: Elizabeth Bolarinwa
Person Months Worked: 2.00 **Funding Support:**
Project Contribution:
International Collaboration:

International Travel:
National Academy Member: N
Other Collaborators:

Participant Type: High School Student
Participant: Tristan Meier
Person Months Worked: 2.00 **Funding Support:**
Project Contribution:
International Collaboration:
International Travel:
National Academy Member: N
Other Collaborators:

Participant Type: High School Student
Participant: Olivia Zapfe
Person Months Worked: 2.00 **Funding Support:**
Project Contribution:
International Collaboration:
International Travel:
National Academy Member: N
Other Collaborators:

Participant Type: Undergraduate Student
Participant: Gina Disalvo
Person Months Worked: 1.00 **Funding Support:**
Project Contribution:
International Collaboration:
International Travel:
National Academy Member: N
Other Collaborators:

ARTICLES:

Publication Type: Journal Article Peer Reviewed: Y **Publication Status:** 4-Under Review
Journal: ACS Applied Materials & Interfaces
Publication Identifier Type: Publication Identifier:
Volume: Issue: First Page #:
Date Submitted: Date Published:
Publication Location:
Article Title: Self-assembly of DNA-Minocycline Complexes by Metal Ions with Controlled Drug Release
Authors: Ting Zhang, Jia Nong, Nouf Alzahrani, Zhicheng Wang, Tristan Meier, Dong Gyu Yang, Yonggang Ke, Y
Keywords: DNA nanostructure, minocycline, DNA-minocycline assembly, drug release
Abstract: Here we reported a study of metal ions-assisted assembly of DNA-minocycline (MC) complexes and their potential application for controlling MC release. In the presence of divalent cations of magnesium or calcium ions (M2+), MC, a zwitterionic tetracycline analogue, was found to bind to phosphate groups of nucleic acids via an electrostatic bridge of phosphate (DNA)-M2+-MC. We investigated multiple parameters for affecting the formation of DNA-Mg2+-MC complex, including metal ion concentrations, base composition, DNA length, and single- versus double-stranded DNA. The reported study of metal ion-assisted DNA-MC assembly not only increased our understanding of biochemical interactions between tetracycline molecules and nucleic acids, but also contributed to the development of a highly tunable drug delivery system to mediate MC release for clinical applications.
Distribution Statement: 1-Approved for public release; distribution is unlimited.
Acknowledged Federal Support: **Y**

RPPR Final Report
as of 08-Feb-2019

Publication Type: Journal Article Peer Reviewed: **Publication Status:** 4-Under Review
Journal: Small
Publication Identifier Type: Publication Identifier:
Volume: Issue: First Page #:
Date Submitted: Date Published:
Publication Location:
Article Title: Bio-mimetic Compartments Scaffolded by Nucleic Acid Nanostructures
Authors: Jinglin Fu, Sung Won Oh, Kristin Monckton, Georgia Arbuckle-Keil, Yonggang Ke and Ting Zhang
Keywords: DNA-scaffolded assembly, DNA nanocaged enzyme, DNA-confined lipid membrane, smart drug delivery, synthetic cell
Abstract: The behaviors of living cells are governed by a series of regulated and confined biochemical reactions. The design and successful construction of synthetic cells can be useful in a broad range of applications that will bring significant scientific and economic impact. Over the past few decades, DNA self-assembly has enabled the design and fabrication of sophisticated 1D, 2D and 3D nanostructures, and has been applied to organizing a variety of biomolecular components into prescribed 2D and 3D patterns. In this “Concept”, we focus on the recent and exciting progress in DNA-scaffolded compartmentalizations and their applications in enzyme encapsulation, lipid membrane assembly, artificial transmembrane nanopores and smart drug delivery. Taking advantage of these features promises to deliver breakthroughs toward the attainment of new synthetic cells and sub-cellular components.
Distribution Statement: 1-Approved for public release; distribution is unlimited.
Acknowledged Federal Support:

DISSERTATIONS:

Publication Type: Thesis or Dissertation
Institution: Rutgers University-Camden
Date Received: 16-Oct-2017 Completion Date: 9/1/17 9:12PM
Title: EXPLORING GLOBAL AND MICRO-ENVIRONMENT CONDITIONS FOR AFFECTING ENZYME ACTIVITIES AND FUNCTIONAL TRANSITIONS
Authors: John Collins
Acknowledged Federal Support: **Y**

Publication Type: Thesis or Dissertation
Institution: Rutgers-Camden
Date Received: 05-Feb-2019 Completion Date: 5/1/18 4:00AM
Title: Co-aggregation Studies of Nucleic Acid Nanostructures with Tetracycline Molecules
Authors: Nouf Alzahrani
Acknowledged Federal Support: **N**

Publication Type: Thesis or Dissertation
Institution: Rutgers University-Camden
Date Received: 05-Feb-2019 Completion Date: 5/1/18 4:00AM
Title: DNA-PROTEIN HYBRID NANOSTRUCTURES AND ITS FUNCTIONAL APPLICATION
Authors: Samirah Ghalib
Acknowledged Federal Support: **N**

RPPR Final Report
as of 08-Feb-2019

PATENTS:

Intellectual Property Type: Patent Date Received: **05-Feb-2019**
Patent Title: DNA Logic-gated Proximity Assembly Circuit for Biochemical Sensing
Patent Abstract: This application relates to nucleic acid-based sensors, kits 5 that include such sensors, and met
Patent Number: 62/647,014
Patent Country: USA
Application Date: 23-Mar-2018 Application Status: 1
Date Issued:

Intellectual Property Type: Patent Date Received: **05-Feb-2019**
Patent Title: DNA-CROWDED ENZYME COMPLEX WITH CONTROLLED SPATIAL CONFINEMENT
Patent Abstract: This application provides nucleotide-crowded macromolecular complex compositions and methc
Patent Number: 62/482,882
Patent Country: USA
Application Date: 07-Apr-2017 Application Status: 1
Date Issued:

Developing Regulatory Biochemistry Reaction Circuits

Principal Investigator: Jinglin Fu
Rutgers University-Camden

Reporting period: 8/01/14-7/31/18
Proposal Number: 65330LSYIP
Agreement Number: W911NF1410434

I. Scientific and Technical Objectives

Statement of objectives: The proposed research will apply the organizational power of DNA nanotechnology to the challenges of engineering biochemical reaction circuits with regulatory and feedback functions. The specific aims are: (1) Design and construct aptamer lock-controlled DNA nanotweezers that switch conformations upon binding to target pathway molecules. (2) Use designed DNA nanotweezers to assemble multienzyme pathways that can be regulated through feedback of product generation or substrate consumption. (3) Develop logic-gated "swinging arms" to channel the transfer of intermediates in multienzyme pathways for controlling pathway activity and specificity in response to molecular inputs. (4) Construct an artificial electron-transport chain to facilitate electron transfer along a redox potential gradient within the reaction pathway.

Methods to be employed: DNA nanostructures with specific geometries will be designed and used as the assembly platforms for integrating regulatory circuits, nanomechanical properties and multienzyme pathways. In order to modulate reaction kinetics, two regulatory mechanisms of aptamer-based molecular locks and logic-gated swinging arms will be designed to regulate the spatial interactions between catalytic components for activating or inhibiting the specific enzyme pathway activity. Structural characterization and enzyme activity measurements will be employed to determine the critical parameters for assembling functional reaction pathways with high yield.

Technical Aims

AIM 1: Design and construct aptamer lock-controlled DNA nanostructures. We will use aptamers to construct molecular locks that are able to switch conformations upon binding to target small molecules including enzyme cofactors and metal ions. The aptamer locks will be implemented into DNA nanotweezers to regulate the spatial distance between arms. This aim will lay the structural and chemical foundations for feedback regulation.

AIM 1-1. Select and characterize aptamers that bind to enzyme cofactors and metal ions.
AIM 1-2. Design and construct aptamer-based molecular locks that will switch conformations upon binding to target molecules.
AIM 1-3. Integrate the aptamer locks into DNA tweezers to regulate the spatial distance between arms.

AIM 2: Engineer feedback-regulated enzyme systems. We will apply the aptamer-switchable DNA nanostructures to the assembly and regulation of enzyme/cofactor pairs and enzyme pathways. Aptamer locks will sense the presence of cofactors and the external effectors and thereby induce a conformation change in the DNA structures to regulate the distance between enzyme and cofactor, or enzyme pairs. The switchable spatial interaction will activate or inhibit

the function of the enzyme systems, which will realize the feedback regulation of enzyme activities in response to the level of reaction substrates, products or effectors.

AIM 2-1. Assemble enzyme and cofactors onto DNA structures and evaluate the spatial parameters that govern activity.
AIM 2-2. Engineer feedback-regulated enzyme reactions in response to external effectors, and cofactors that are consumed (substrates) or generated (products) by the reaction.
AIM 2-3. Feedback regulation of a multienzyme pathway in response to both the reaction intermediates and final products.

AIM 3: Develop logic-gated multienzyme pathway circuits. We will design and engineer swinging arms to channel intermediate in multienzyme pathways. A logic-gated circuit will be incorporated to control the release and activation of swinging arms. In this way, the pathway activity and specificity will be regulated by input DNA strands that trigger the activation of the logic-gated system.

AIM 3-1. Design and construct swinging arm-channeled enzyme pathways.
AIM 3-2. Engineer logic-gated swinging arms.
AIM 3-3. Design and construct logic-gated control of pathway activities and specificities.
AIM 3-4. Develop a tandem logic gate circuit to control a four-enzyme pathway.

AIM 4: Design and construct an artificial electron-transport chain. We will use DNA nanostructures to organize redox cofactors to construct a redox potential gradient. This will guide the electrons from low redox potential to high redox potential within a reaction pathway.

AIM 4-1. Bioconjugation of redox cofactors to DNA molecules.
AIM 4-2. Assemble redox cofactors onto DNA structures and evaluate the spatial parameters that govern electron transfer efficiency.
AIM 4-3. Optimize the geometric arrangements for more efficient and stable electron transfer.

Split AIMS Between YIP and PECASE: The three-year YIP project will demonstrate the proof of concept for aptamer lock-controlled DNA nanostructures that sense NAD and ATP (**Aim 1**) and feedback-regulated enzyme reactions (**Aims 2-1 and 2-2**). The PECASE project will extend **Aim 1 and 2** to explore additional feedback mechanisms (**Aim 2-3**), as well as completing **Aims 3 and 4** to develop logic-gated multienzyme pathways and the artificial electron-transport chain.

II. Concise Accomplishments

(1) *DNA-mediated proximity assembly circuit for actuating biochemical reactions*: We have designed and constructed dynamic DNA nanostructures to control the proximity assembly of catalytic components for actuating biochemical reactions. The actuated biochemical reaction is used to detect various targets. These proximity assembly circuits can be readily extended to a low-cost, rapid and portable system, e.g. paper-based detection, which can be applied to point-of-care diagnosis.
(2) *DNA crowded-enzyme complexes with enhanced activities*: We have developed a simple and robust strategy for the DNA nanocage-templated encapsulation of metabolic enzymes with high assembly yield and controlled packaging stoichiometry. The DNA nanocaged enzyme and DNA-crowded enzyme complex were found to boost and stabilize enzyme activity.
(3) *Activity transition of dehydrogenase:* We have investigated how environmental conditions and short peptides affect enzyme functions, especially, transformed activities. In one example, the Fu group reported a hidden transhydrogenase activity of a diaphorase (DI) by stabilizing the

reduced state of a bound cofactor under anaerobic conditions. In another study, we observed a functional transition from dehydrogenase activity to oxidase activity for a FMN-DI that happened during the long-term storage process. These results can be applied to the design of a versatile toolbox for modulating enzyme functions, and the development of bio-electroactive, NAD-dependent dehydrogenase pathway for production of biofuels and biochemicals.

III. Expanded Accomplishments

III-(1). DNA-mediated proximity assembly circuit for actuating biochemical reactions

We designed a robust and smart DNA nanodevice capable of sensing various bio-targets and reporting an easy-to-read signal. The nanodevice combines the mechanisms of DNA logic-gated structure (sensing unit) with the proximity assembly of enzyme/cofactor system (assembly unit). The assembled system catalyzes a biochemical reaction to produce colorimetric or fluorescence signals. Compared with the commonly used fluorophore/quencher system, the actuated reaction will produce more detectable signal overtime.

a. Design of DNA-mediated proximity assembly of an enzyme/cofactor pair: As shown in **Figure 1a**, our design rationale is based on a DNA-mediated proximity interaction of an enzyme/cofactor system. A catalytic cofactor (e.g. β-nicotinamide adenine dinucleotide, NAD^+; adenosine triphosphate, ATP) is first locked within a DNA hairpin structure with the inhibited accessibility to enzymes, resulting in almost no activity. The opened hairpin allows a cofactor to interact with an enzyme, but only exhibiting low activity due to the poor mass transport of free diffusion in solution. To actuate the reaction, the enzyme and the cofactor are co-assembled onto a dsDNA with proximity-boosted activities. To test the design, we first evaluated activities of different DNA structure-mediated enzyme/cofactor reactions. As shown in **Figure 1b**, a co-assembled enzyme/cofactor pair (glucose-6-phosphate dehydrogenase (G6PDH) and NAD^+) was 100-fold more active than a DNA hairpin-locked cofactor and was also higher than a partially hairpin-opened cofactor and a fully opened and exposed cofactor. This

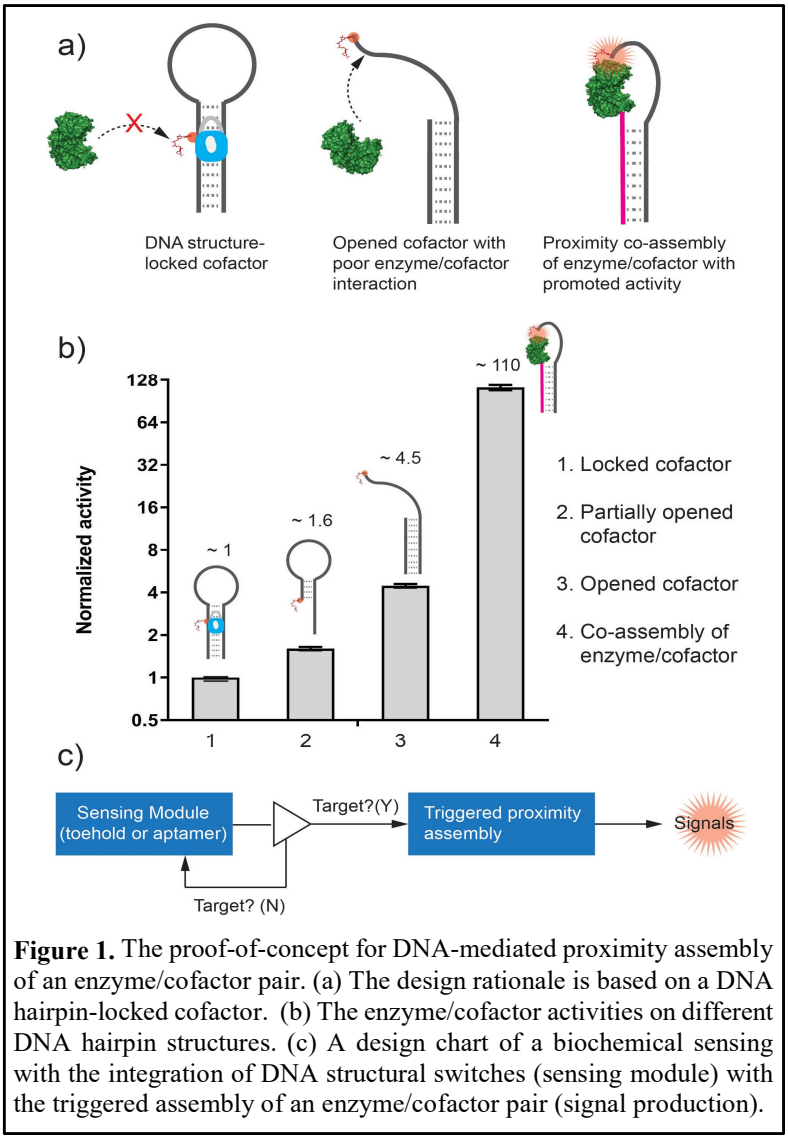

Figure 1. The proof-of-concept for DNA-mediated proximity assembly of an enzyme/cofactor pair. (a) The design rationale is based on a DNA hairpin-locked cofactor. (b) The enzyme/cofactor activities on different DNA hairpin structures. (c) A design chart of a biochemical sensing with the integration of DNA structural switches (sensing module) with the triggered assembly of an enzyme/cofactor pair (signal production).

result provided a foundation of designing a biochemical sensing circuit, where a sensing module of DNA structural switches is used to trigger the assembly of an enzyme/cofactor pair to catalyze a reaction for producing detectable signals (**Figure 1c**).

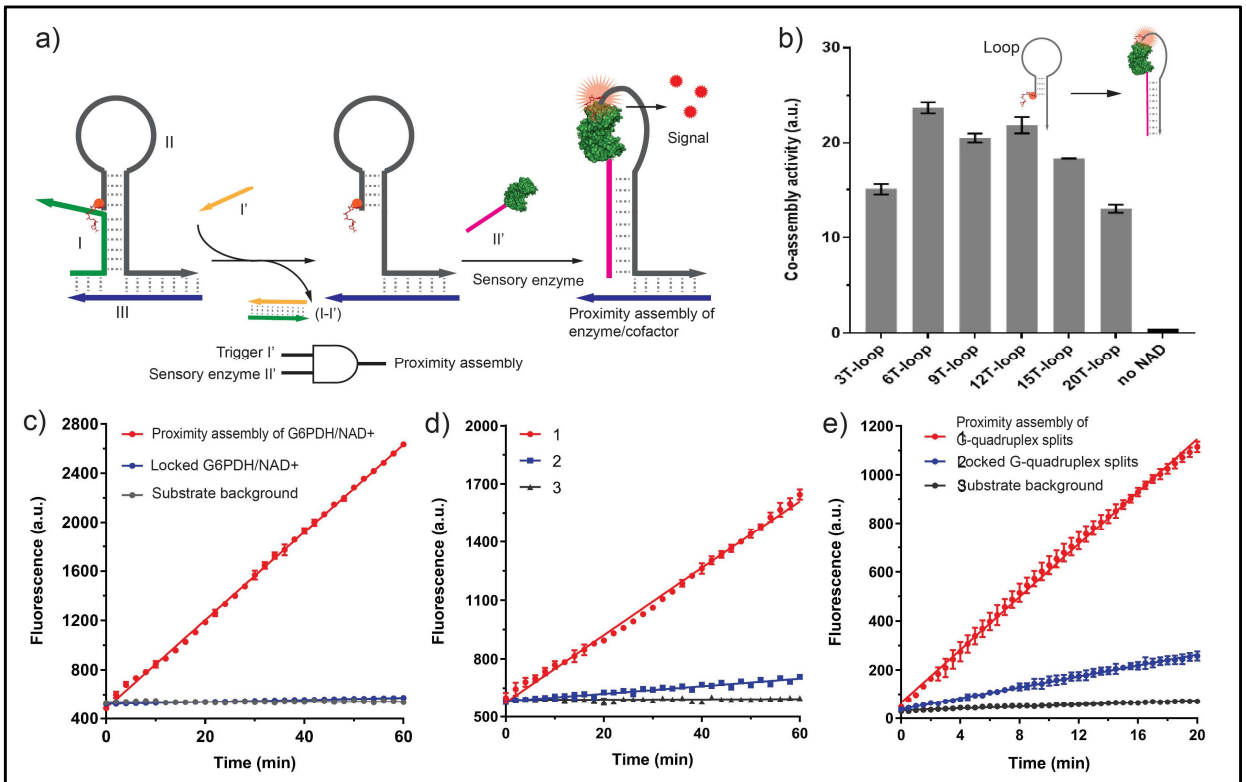

Figure 2. DNA logic-gated assembly of biochemical reactions. (a) A DNA "AND" gated mediation of an enzyme/cofactor pair. (b) Optimization of the hairpin loop length for maximizing the activity performance of the assembled enzyme/cofactor pairs. The assay was monitored for one hour. The DNA logic-gated assembly was used to mediate (c) a glucose-6-phosphate dehydrogenase (G6PDH)/NAD^+ pair, (d) a hexokinase (HEK)/ATP pair and (e) a G-quadruplex/hemin complex. Error bar: range of data from three replicates.

Next, we designed a DNA logic-gated assembly of an enzyme/cofactor pair. As shown in **Figure 2a**, a DNA hairpin structure is composed of a toehold strand (I), a hairpin strand (II) and a base strand (III). An enzyme cofactor (e.g. NAD^+) is conjugated to the 5' end of the hairpin strand. A trigger strand (I') can hybridize with the exposed toehold region (green color) of the strand (I) and displace it from the hairpin structure, resulting in a partially opened structure with a newly exposed region. Then, an enzyme (e.g. G6PDH) conjugated with a strand (II') will recognize this newly exposed region and hybridize with the hairpin strand (II) to produce a co-assembled enzyme/cofactor, which can actuate a reaction to produce colorimetric signals. The overall assembly of the enzyme and the cofactor is controlled by an "AND" gate with the inputs of both a trigger strand (I') and a sensory enzyme (II'). The assembly of DNA logic-gated structure was characterized by polyacrylamide gel electrophoresis (PAGE). The base strand (III) was used to stabilize the hybridization of a toehold strand (I) and a hairpin strand (II), and to reduce the nonspecific assembly of an enzyme and a cofactor. To optimize the performance of the enzyme/cofactor pair, we adjusted the length of the hairpin loop region from 3 T to 20 T and conjugated them to NAD^+ cofactor for reacting with the enzyme. As shown in **Figure 2b**, the loop length from 6 T to 12 T gave the highest activity of co-assembled enzyme/cofactor pair. An optimized length of a ssDNA-linked cofactor provides the flexibility for mapping the enzyme

surface to reach the active site, but does not significantly decrease the local cofactor concentration. To test the versatility, we used the DNA-locked cofactor structure to mediate the proximity assembly of multiple biochemical reactions, including a G6PDH/NAD^+ pair (**Figure 2c**, ~ 53-fold enhancement) and a hexokinase (HEK)/ATP pair (**Figure 2d**, ~ 10-fold enhancement). We also tested the assembly of a complete G-quadruplex/hemin from two split halves (**Figure 2e**, ~ 5.6-fold enhancement). Among these reactions, G6PDH/NAD^+ assembly gave the highest activity enhancement (> 50-fold) shown by a simple fluorescence assay. Thus, this enzyme/cofactor system was chosen for sensing biochemical targets in later studies.

b. Detection of microRNA and adenosine using designed DNA proximity assembly circuits: Due to the low activity of a locked cofactor, it can be pre-mixed together with an enzyme and a substrate solution as a sensing agent. As shown in **Figure 3a**, a simple assay was performed by adding an analyte into this sensing solution for triggering the activation of an enzyme/cofactor reaction. We first tested the detection of a microRNA 21 (hsa-miR-21), which is one of the most frequently upregulated miRNAs in solid tumors, such as breast cancer. As shown in **Figure 3b**, a DNA toehold displacement was designed to recognize hsa-miR-21 sequence, which subsequently triggered the co-assembly of an enzyme/cofactor reaction. As shown in **Figure 3c and d**, the

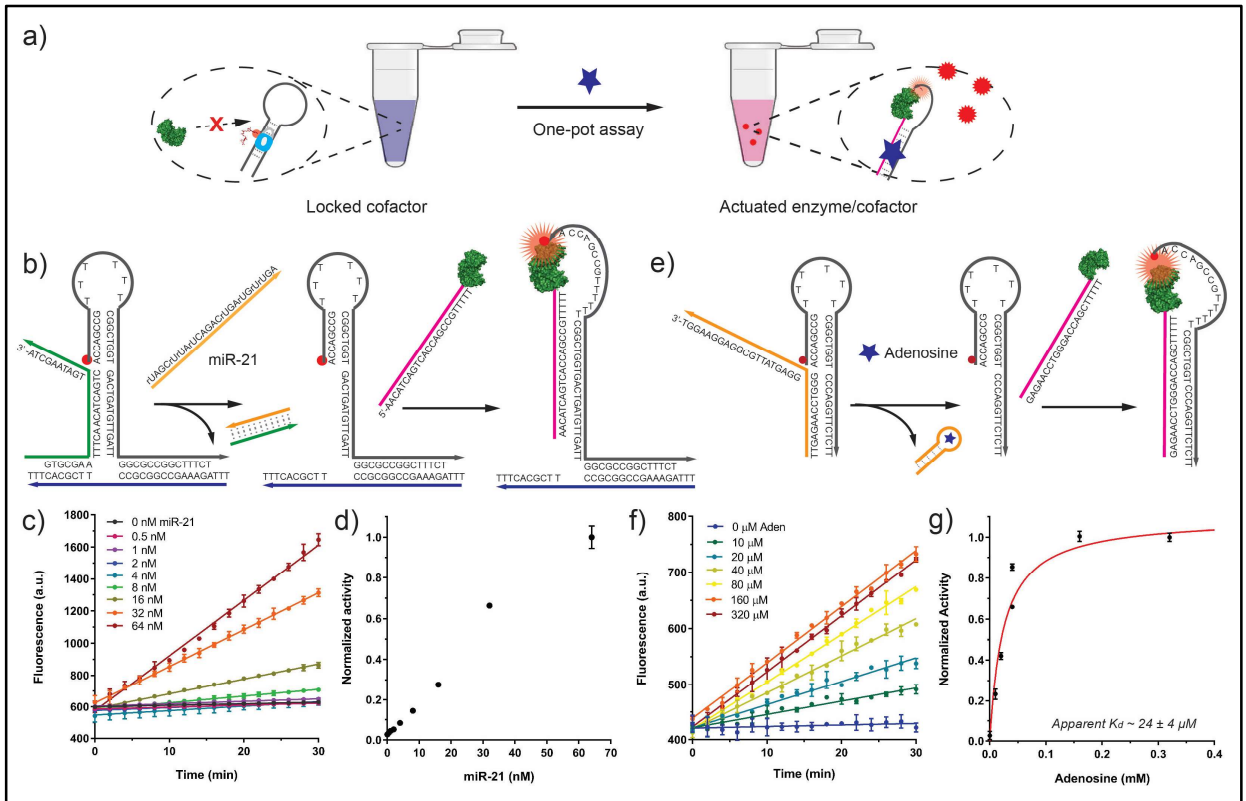

Figure 3. The detection of bio-targets with DNA-mediated assembly circuit. (a) One-pot assay of bio-targets with the actuated enzyme reaction (b) A DNA hairpin with the toehold displacement for detecting hsa-miR-21, (c) the actuation of G6PDH/NAD^+ reactions depending on the addition of hsa-miR-21 from 0 to 64 nM, and (d) the activities of G6PDH/NAD^+ pairs depending on the addition of miRNA. The activities are normalized to the reaction of 64 nM miR-21. (e) An aptamer-locked hairpin for detecting adenosine, (f) the actuation of G6PDH/NAD^+ reactions depending on the addition of adenosine from 0 to 320 μM, and (g) the activities of G6PDH/NAD^+ pairs depending on the addition of adenosine. The activities are normalized to the reaction of 0.32 mM adenosine. The concentrations of DNA hairpin-locked cofactors and enzymes are 100 nM. The apparent dissociation constant (K_d) of aptamer-locked sensor is ~ 24 ± 4 μM. Error bar: range of data from three replicates.

activity of G6PDH/NAD^+ reaction was proportional to the added concentration of hsa-miR-21. A detection limit of ~ 1 nM miRNA was estimated based on 3× SD, where SD is the standard deviation of three reaction slopes for blank samples. Alternatively, an aptamer switch can be incorporated into the DNA hairpin structures for responding to small molecules. As shown in **Figure 3e**, adenosine aptamer (Ade-Apt) was used to lock the hairpin structure with a stem region of a 11-bp aptamer-complement duplex. Upon the addition of adenosine, the adenosine-aptamer binding will induce a conformational switch, resulting in a subsequent assembly of enzyme and cofactor similarly as described in Figure 2. To facilitate the aptamer switch induced by the adenosine binding, a base strand was not used for stabilizing aptamer-hairpin hybridization. A titration curve showed that the activity of G6PDH/NAD+ pair was increased corresponding to the concentration of adenosine from 0 – 320 μM (Figure 3f-g). The detection limit was estimated to be < 10 μM based on the definition of 3 × SD. The apparent dissociation constant (K_d) of the aptamer-locked cofactor was ~ 24 ± 4 μM. Additionally, the sensitivity of the aptamer circuit can be tuned by increasing the length of aptamer-complement duplex. For example, the detection limit of the adenosine sensor was increased to ~ 400 μM by using a base strand to stabilize aptamer-hairpin hybridization. The apparent K_d of the aptamer-locked cofactor was increased ~ 2.5 ± 0.5 mM. This opens a possibility of engineering a series of sensors with different ranges of sensitivity.

c. The DNA hairpin assembly-amplified enzyme/cofactor pairs for increasing signal production: To increase the signal production, a DNA hairpin assembly circuit was used to bring together multiple enzyme/cofactor pairs by just one trigger molecule. As shown in **Figure 4a**, a sensing circuit first releases a trigger strand upon recognizing a target. Then, the trigger strand induces the assembly of hairpin substrates into either a long duplex by hybridization chain reaction (HCR), or produces many short duplexes by catalytic hairpin assembly (CHA). The assembled hairpin structures are able to anchor multiple pairs of enzymes and cofactors. The gain of this signal production can be estimated by multiplying the assembled enzyme/cofactor pairs ($N_{hairpin\ assembly}$) and the boosted activity of an enzyme/cofactor pair ($F_{enzyme/cofactor}$). As shown in **Figure 4b**, a reported CHA circuit was used to produce short DNA duplexes displaying a probe (probe 'a') which could trigger the assembly of a pair of DNA hairpin-locked cofactor and enzyme through strand displacement As shown in **Figure 4c**, native PAGE was used to characterize the CHA-produced short DNA duplexes by titrating the trigger strand from 0.1 nM to 100 nM. The band-shifts of DNA gel showed that almost all hairpins (100 nM) were assembled into short duplexes at the addition of 10 nM trigger strand. These CHA-produced duplexes were also validated to react with a toehold locked hairpin by Foster resonance energy transfer (FRET), where a Cy3 was labelled on a locked hairpin, and a Cy5 was labelled on an enzyme-DNA strand. The assembly of a locked hairpin and an enzyme-DNA strand was triggered by CHA-produced duplexes with increased Cy3-Cy5 FRET signals (**Figure 4c**, right panel). More gel characterizations were shown in Supplementary Figure S11. As shown in Figure 4d, we tested the activity of a G6PDH/NAD^+ pair by titrating the concentrations of added trigger strands. A nonspecific enzyme activity was observed without the addition of any trigger strand due to the assembly leakage of CHA circuit. The increases in enzyme activities were detected with the addition of the trigger strand from 0.1 nM to 100 nM, in which the enzyme activity was close to the saturated activity when the trigger strand was > 10 nM, due to the amplification of assembled enzyme/cofactor structures. This result was consistent with the PAGE characterization in Figure 4c. Using this CHA assembly circuit, we were able to detect 0.1 nM miR-21 with a signal-to-noise ratio > 3. This detection limit of CHA assembly circuit of enzyme/cofactor pairs was one magnitude lower than the toehold-mediated assembly of enzyme/cofactors (Figure 3b).

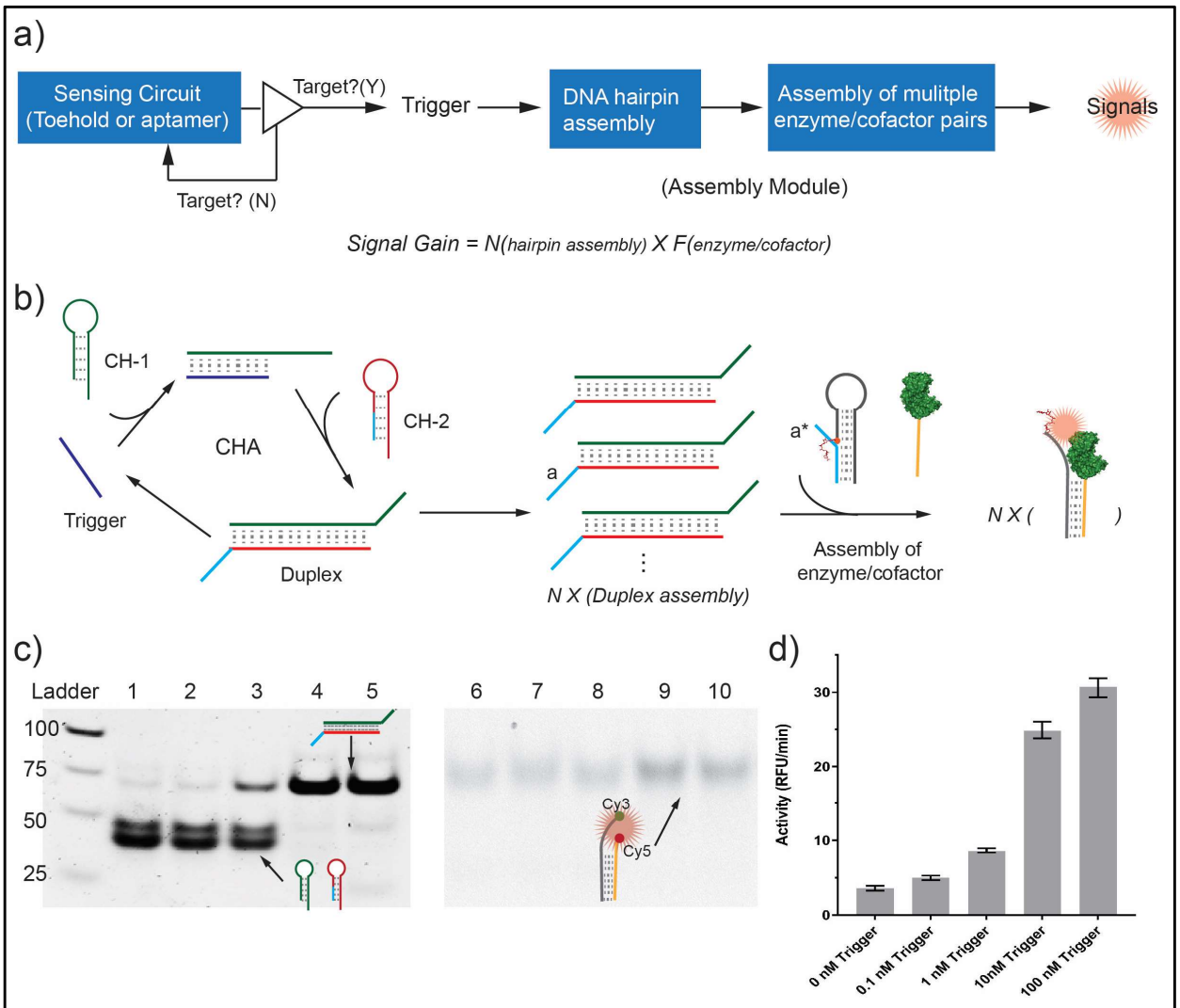

Figure 4. The DNA hairpin assembly-mediated actuation of enzyme/cofactor pairs for increasing the detection sensitivity. (a) The design concept of using DNA hairpin assembly to assemble multiple enzyme/cofactor pairs with one trigger molecule. (b) The CHA is used to produce short DNA duplexes for assembling multiple G6PDH/NAD^+ pairs: T, trigger strand. (c) Left panel: Native PAGE for characterizing the CHA production of duplexes. Lane 1: 100 nM mixture of CH-1 and CH-2 hairpins; Lane 2-5: 100 nM mixture of CH-1 and CH-2 with the addition of 0.1 nM (lane 2), 1 nM (lane 3), 10 nM (land 4) and 100 nM (lane 5) trigger strands. Right panel (lane 6-10): Cy3-Cy5 fluorescence gel for the product of lane 1-5 incubating with 100 nM DNA hairpin-locked NAD^+ (Cy3 label) and G6PDH strand (Cy5 label). (d) The G6PDH/NAD^+ activities depending on the addition of trigger strands from 0 – 100 nM. Error bar: range of data from three replicates.

d. Conclusion and Significance: In summary, we have demonstrated a nanoscale molecular circuit to control the proximity assembly of enzyme/cofactor pairs. A DNA hairpin structure was used to lock a catalytic cofactor for the inhibition of an enzyme/cofactor interaction. The locked cofactor hairpins were incorporated with the mechanisms of toehold displacement and aptamer switch for sensing target molecules and triggering the subsequent assembly of an enzyme and a cofactor, which actuated a biochemical reaction to produce detectable signals. It is also possible to use DNAzyme to replace enzyme/cofactor for producing signals. The DNA proximity assembly circuit only consisted of a few ssDNA strands and could be engineered to detect various molecular targets.

III-(2) An Activity Transition of Dehydrogenase

We have investigated how environmental conditions and short peptides affect enzyme functions, especially, transformed activities. In one example, the Fu group reported a hidden transhydrogenase activity of a diaphorase (DI) by stabilizing the reduced state of a bound cofactor under anaerobic conditions. This enzyme was demonstrated to catalyze the hydride transfer between NAD(P)H and $NAD(P)^+$. In another study, the Fu group observed a functional transition from dehydrogenase activity to oxidase activity for a FMN-DI that happened during the long-term storage process. The enzyme did not simply lose its activity but obtained a new oxidase activity during the denaturation. This activity transition was attributed to the alternation of binding strength of a cofactor with a protein.

Diaphorase (DI) is commonly used as a NAD(P)H dehydrogenase that catalyzes the electron transfer from a NAD(P)H to a variety of electron acceptors, such as methylene blue, resazurin, vitamin K_3 and dichlorophenolindophenol (**Figure 5A**). The redox center of a DI protein is a bound flavin monucleotide (FMN) that accepts two electrons from NADH, and is reduced to a $FMNH_2$ (**Figure 5B**). The reduction of a FMN-DI to a $FMNH_2$-DI can be characterized by the reduced absorbance at ~ 452 nm (**Figure 5C**). FMN-containing DI was also reported to behave as a NADH oxidase where the reduced $FMNH_2$-DI was oxidized by molecular oxygen to produce hydrogen peroxide. However, few reports have carefully studied how the dehydrogenase activity was correlated to the oxidase activity for a FMN-DI. Here, we report a transformed activity of a FMN-bound DI from a primary dehydrogenase to a primary oxidase that happened during the storage denaturation of protein. The alteration of the binding strength of a FMN cofactor to a DI protein was suggested to be responsible for the observed functional switch of the enzyme.

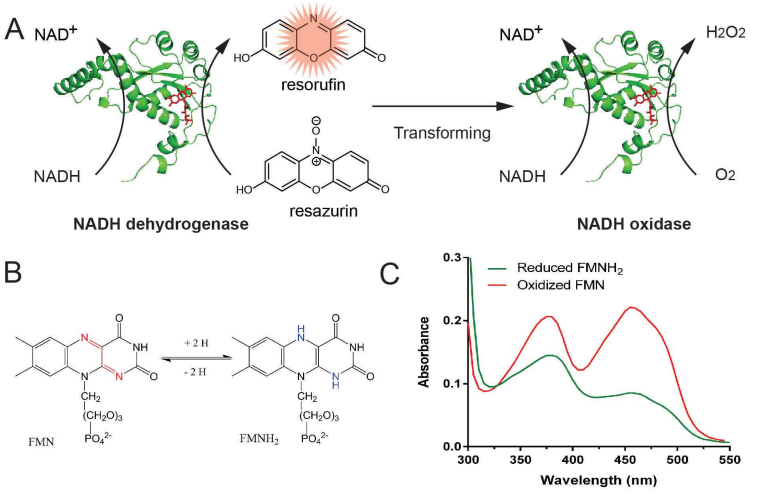

Figure 5. (A) Schematic illustration of the transformed activity of a FMN-DI from a NADH dehydrogenase to a NADH oxidase during the denaturation. (B) The redox center of a FMN cofactor accepts two electrons for reducing to a FMNH2. (C) The decreased absorbance at 455 nm due to the reduction of FMN-DI to FMNH2-DI.

a. Hidden Transhydrogen Activity of A FMN-Bound Diaphorase under Anaerobic Conditions.: As shown in **Figure 6**, a 20 μM solution of FMN-DI was first reduced to $FMNH_2$-DI by adding 20 μM NADH. In regular aqueous solution containing dissolved oxygen, $FMNH_2$-DI was quickly oxidized back to FMN-DI with the simultaneous reduction of oxygen to H_2O_2, thus resulting in the increased absorbance at 452 nm. To stabilize the reduced state of $FMNH_2$-DI, dissolved oxygen was removed by purging the aqueous buffer solution with pure argon gas (20 psi, 30 min). Under this anaerobic condition, $FMNH_2$-DI maintained a stable reduction state with a low absorbance at 452 nm. We hypothesized that FMN-DI, with the stabilized reduction state,

might perform as a transhydrogenase which catalyzes the hydride exchange between a NADPH and a NAD^+ (or vice versa).

$$NADH + FMN\text{-}DI \rightleftharpoons NAD^{\oplus} + FMNH_2\text{-}DI$$
$$FMNH_2\text{-}DI + NADP^{\oplus} \rightleftharpoons FMN\text{-}DI + NADPH \quad (1)$$

As shown in **Scheme 1**, FMN-DI serves as a redox center to catalyze the reversible transfer of hydrides. To test this, analogues of thio-NAD^+ and thio-$NADP^+$ were used to characterize the transhydrogen reaction. As shown in **Figure 7A**, a thio-NAD^+ analogue resembles the structure of a NAD^+, except for a thio-ester substitution at the nicotinamide group, which exhibits a red-shifted absorbance for reduced thio-NADH at ~ 400 nm. This shifted absorbance of thio-NADH is easily distinguishable from the 340 nm absorbance of NAD(P)H (**Figure 7A**). We first compared the substrate activity of the two analogues of thio-NAD^+ and thio-$NADP^+$ for FMN-DI. It was found that thio-$NADP^+$ was much less active than thio-NAD^+ for FMN-DI. Further kinetics study showed that FMN-DI exhibited a much smaller k_{cat} for thio-$NADP^+$ than that for thio-NAD^+. Thus only thio-NAD^+ was used as a reporter for characterizing the transhydrogen reaction. As shown in **Figure 7B**, the increased absorbance at 400 nm was observed for the DI-catalyzed transhydrogen reaction between NADH and thio-NAD^+, as well as between NADPH and thio-NAD^+. As a negative control, the incubation of thio-NAD^+ with NADH or NADPH did

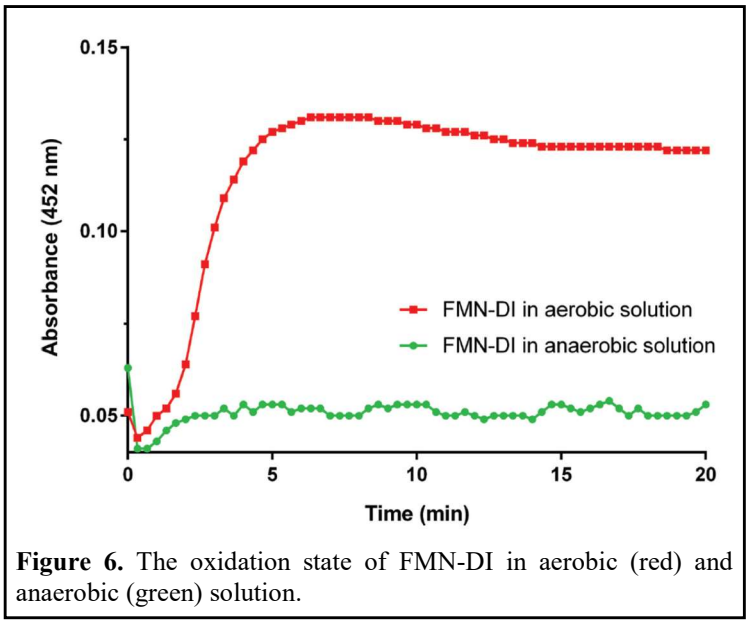

Figure 6. The oxidation state of FMN-DI in aerobic (red) and anaerobic (green) solution.

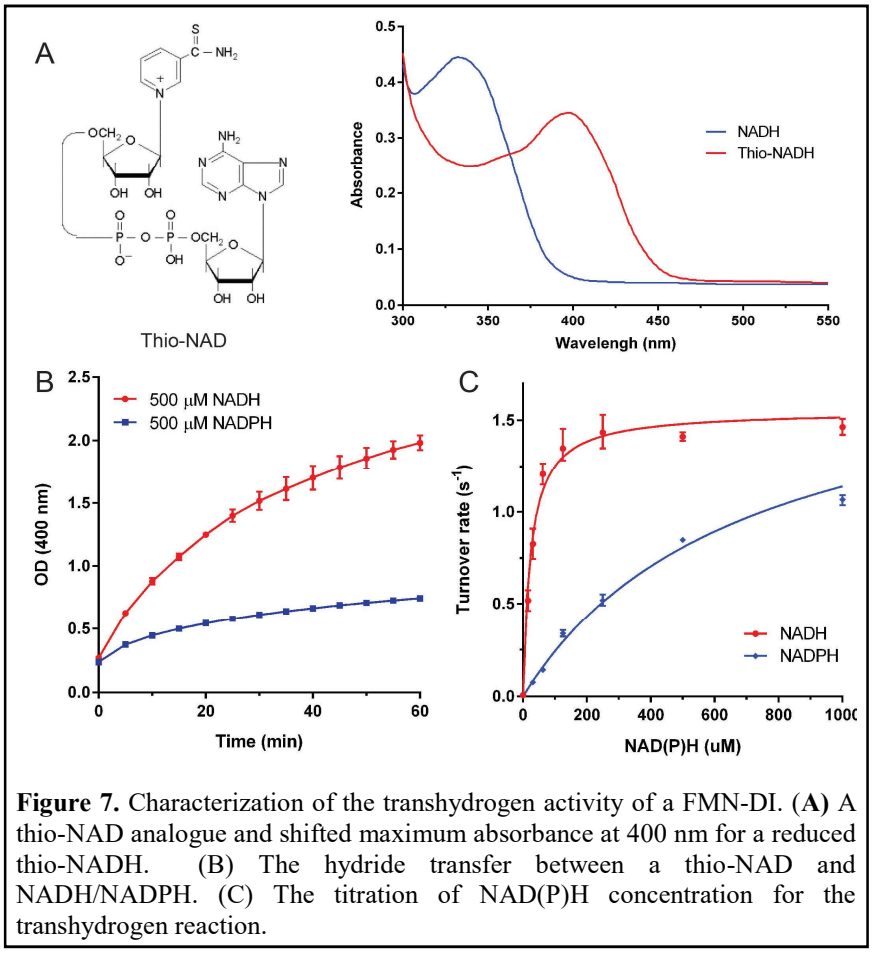

Figure 7. Characterization of the transhydrogen activity of a FMN-DI. (**A**) A thio-NAD analogue and shifted maximum absorbance at 400 nm for a reduced thio-NADH. (B) The hydride transfer between a thio-NAD and NADH/NADPH. (C) The titration of NAD(P)H concentration for the transhydrogen reaction.

not result in a significant increase of absorbance at 400 nm. Another control experiment also showed that the addition of free FMN molecules could not enhance the rate of the transhydrogen reaction. All of these results suggested that the DI-bound FMN cofactor was responsible for catalyzing the transhydrogen reaction, not the unbound and freely diffused FMN. FMN-DI was further found to discriminate between NADH and NADPH, which catalyzed the reaction between NADH and thio-NAD^+ 3-fold faster than the reaction between NADPH and thio-NAD^+. Detailed kinetic analysis showed that FMN-DI exhibited similar turnover numbers between NADH (a k_{cat} value of ~ 1.64 ± 0.05 s^{-1}) and NADPH (a k_{cat} value of ~ 1.93 ± 0.06 s^{-1}). However, the apparent K_m value of NADH (~ 24 ± 3 μM) was much smaller than that of NADPH (~ 699 ± 49 μM) (**Figure 7C**). This suggested that NADPH was bound to the enzyme less efficiently than NADH. Thus FMN-DI might favor the hydride transfer from a high concentration of NADPH to a low concentration of NAD^+.

Using this newly discovered transhydrogenase activity, FMN-DI was demonstrated to allow a NADH-specific lactate dehydrogenase to utilize NADPH as an electron donor, where NADPH was converted to NADH by the DI-catalyzed transhydrogen reaction. We chose a special lactate dehydrogenase (LDH) that reacted with NADH 100-fold faster than NADPH for converting pyruvate to lactate. As shown in **Figure 8A**, we first used a mixture of NADPH and thio-NAD^+, where the DI-catalyzed the hydride exchange from NADPH to thio-NAD+, generating thio-NADH accompanied with an increased absorbance at 400 nm. The sequential addition of LDH induced a quick decrease in the absorbance at 400 nm, indicating the consumption of thio-NADH by LDH. Next, we tested FMN-DI for catalyzing the direct hydride transfer between NADPH and NAD^+. As shown in **Figure 8B**, LDH cannot efficiently use NADPH as an electron donor without the addition of FMN-DI, resulting in a very slow decrease in the absorbance at 340 nm (shown in red). Conversely, the addition of FMN-DI into the reaction mixture catalyzed the hydride transfer from NADPH to NAD^+ with the production of more NADH. Then, the produced NADH was quickly consumed by the LDH with a faster decreased absorbance at 340 nm (shown in black). As another control experiment, FMN-DI was incubated with the mixture of NADPH and NAD^+ without the addition of LDH to consume the produced NADH (shown in green). The absorbance at 340 nm varied slightly over time which was similar to that of the no-enzyme control (shown in blue) because both reduced NADH and NADPH had similar absorbance at 340 nm. Similarly, FMN-DI was also demonstrated to activate a NADH-specific malic dehydrogenase to utilize NADPH for reducing oxaloacetate. The above results demonstrated that

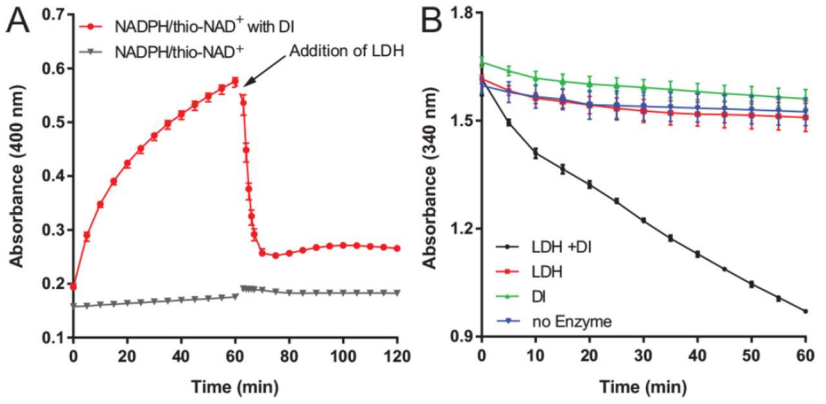

Figure 8. (A) Real-time monitoring of the hydride exchange from NADPH to thio-NAD^+ at 400 nm, and the consumption of thio-NADH with the addition of LDH. (B) The LDH-catalyzed oxidation was activated by the addition of a FMN-DI to convert NADPH to NADH (black) and controls of no addition of DI (red), no addition of LDH (red) and no addition of enzymes (blue). Anaerobic solution was used for the assay. Error bars were generated as the range of at least three replicates.

FMN-DI catalyzed the hydride exchange between NADPH and NAD^+ under anaerobic conditions. Most natural transhydrogenases in living cells under reduced environments favor the transhydrogenation from NADPH to NADH, mainly due to the fact that the physiological ratio of NADPH/$NADP^+$ (~ 60) is much higher than the ratio of NADH/NAD^+ (~ 0.03) and the cellular concentration of NADPH (~ 120 μM) is also higher than that of NADH (~ 80 μM). This study implied that DI could have a new function as transhydrogenase for some organisms, especially for anaerobic species.

b. Observation of increased NADH oxidase activity by the storage denaturation of protein: To characterize the NADH dehydrogenase activity of DI from *G. stearothermophilus*, we used a resazurin assay in which a FMN-DI catalyzed the oxidation of NADH to NAD^+ while concurrently transferring two electrons to a resazurin for reducing it to a strongly fluorescent resorufin. Freshly-made FMN-DI showed a much higher dehydrogenase activity (>20-fold) than the aged FMN-DI solution that has been frequently used and stored at 4 °C for more than a year (**Figure 9A**). This decreased activity was also commonly observed for many other proteins during their storage, which could be induced by a series of factors, such as folding change, aggregation, oxidation, and cofactor damage. However, we accidently discovered that as FMN-DI lost its dehydrogenase activity, it became more active as a NADH oxidase, which used NADH to reduce O_2 to H_2O_2. As shown in **Figure 9B**, the NADH oxidation was characterized by the decreased absorbance at 340 nm. The old FMN-DI solution catalyzed the complete depletion of NADH within 50 min, whereas the freshly-made FMN-DI solution showed very little oxidation of NADH with only slight decreased absorbance at 340 nm. As shown in **Figure 9C**, the production of H_2O_2 during the NADH oxidation was verified by adding horseradish peroxidase (HRP) that used produced H_2O_2 to oxidize Amplex Red to strongly fluorescent resorufin. The formation of C4a-hydroperoxyflavin from the oxidation of reduced FMN is suggested as a key intermediate for producing H_2O_2 according to the previous studies. FMN-DI was also tested for any potential NADH peroxidase activity that could use NADH to reduce H_2O_2. This was performed under the anaerobic condition in which the oxidase activity was inhibited. Different concentrations of FMN-DI solutions from 50 nM to 400 nM were incubated with NADH and H_2O_2. FMN-DI solutions were not observed for significant NADH peroxidase activity. As shown in **Figure 9D**, FMN-DI solution was tested for the transformation from a NADH dehydrogenase to a NADH oxidase activity by incubation at room temperature over seven days. As expected, for the fresh FMN-DI solution (day 0), we observed a strong dehydrogenase activity, and the oxidase activity was very weak. As the enzyme solution was incubated for more days, the oxidase activity increased accordingly. Conversely, the dehydrogenase activity was decreased as incubating for more days. As a control, free FMN molecules showed very little oxidase activity at even high micro-molar concentrations. This result suggested that a FMN-containing DI gradually transformed from a dehydrogenase to an oxidase during the long-term storage under room temperature or elevated temperature.

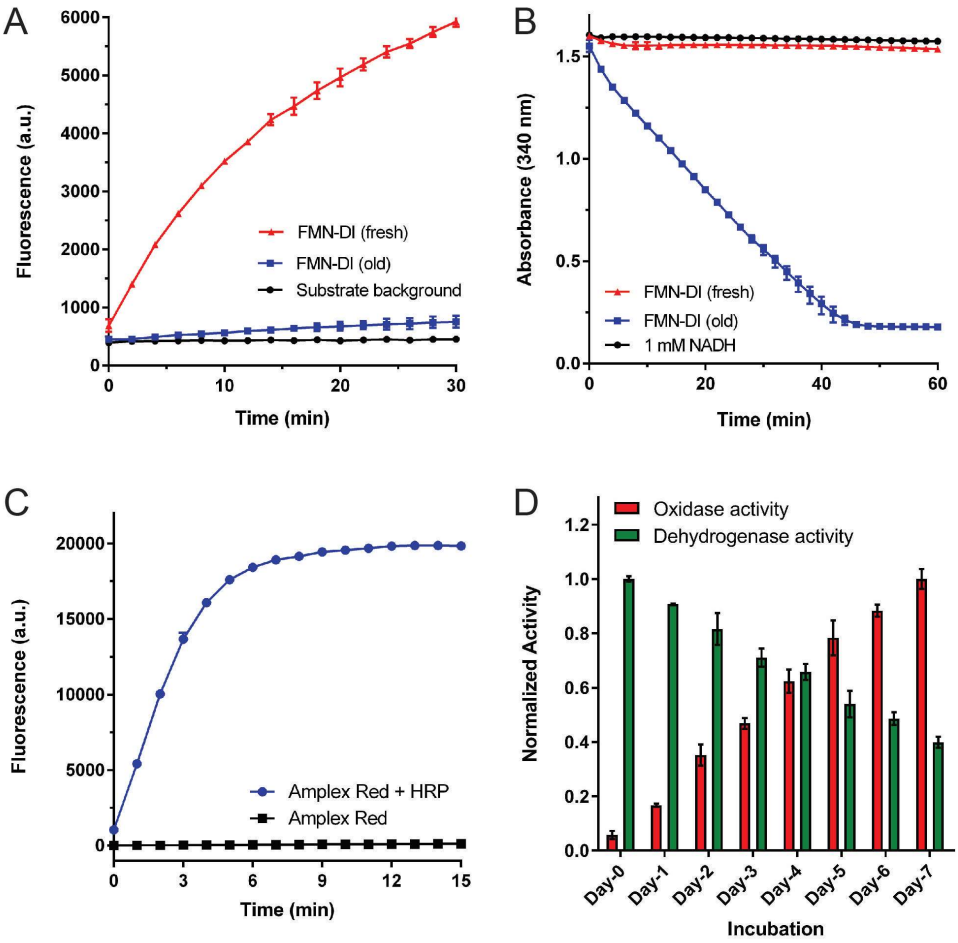

Figure 9. The transformed activities of a FMN-DI during the denaturation. (A) The fresh FMN-DI solution shows a 20-fold higher dehydrogenase activity than a FMN-DI (old) that is stored for more than a year. (B) An increased oxidase activity for an old FMN-DI solution as compared with a fresh FMN-DI solution. (C) The production of H_2O_2 from the oxidation of NADH is confirmed by the addition of HRP and Amplex Red to produce strongly fluorescent resorufin (excitation ~ 532 nm/ emission ~ 590 nm). (D) The transformed activities of a FMN-DI under the incubation at ~ 25 °C in dark.

Different from flavoproteins, such as succinate dehydrogenase, FMN was not covalently linked to a DI, but tightly-bound to the protein. Therefore, we hypothesized that the binding strength between a FMN and a DI protein might influence the observed functional change of the enzyme. The tightly-bound FMN was suggested to be critical for the dehydrogenase activity, and was also less accessible to oxygen molecules that showed more resistance to the aerobic oxidation in aqueous solution (low oxidase activity). Conversely, the binding between a FMN and a DI protein was gradually destabilized during the long-term storage under room temperature. The loosely-bound FMN on DI resulted in the loss of the dehydrogenase activity. However, this dissociated FMN could work as an electron mediator between DI and dissolved molecular oxygen, and the DI exhibited more NADH oxidase activity. To test this hypothesis, we first used molecular weight cut-off filter (3 kD) to wash the solutions of fresh FMN-DI and aged FMN-DI. If FMN is tightly bound with DI, most of FMN molecules will still stay with protein on the top of the filter. If FMN is dissociated from a DI protein, free FMN molecules will pass through the filter membrane. As

shown in **Table 1**, the relative ratio of FMN to DI was characterized using their unique absorbance at 452 nm (FMN) and 280 nm (DI protein). For a fresh FMN-DI solution, the value of $A_{452\ nm}/A_{280\ nm}$ was similar (~ 0.12 – 0.13) even after two washes, indicating that FMN was tightly bound with DI protein. Conversely, for an aged FMN-DI solution (one year old), the value of $A_{452\ nm}/A_{280\ nm}$ decreased from 0.144 to 0.072 after one wash, and was further decreased to 0.048 after two washes. This suggested that FMN was dissociated from DI when DI was stored for a long period.

To measure the binding of FMN with DI, we attempted to add free FMN molecules into the DI protein solution (DI protein with the depletion of most bound FMN) for enhancing dehydrogenase and oxidase activities. As shown in **Figure 10A**, the dehydrogenase activity of a DI protein solution was increased as adding more FMN from 0 to 32 nM, and was almost saturated for FMN > 16 nM. For control, free FMN by itself did not catalyze the hydride transfer between NADH and resazurin. Since FMN-DI has a smaller K_m of ~ 20- 40 μM for NADH, under the high NADH concentration of 1 mM, we assumed that the reaction rate (initial velocity, V) is directly correlated to the concentration of the 'FMN-$DI_{(DH)}$ complex' (FMN-$DI_{(DH)}$ catalyzes the dehydrogenation reaction), where $V \sim k^*[FMN\text{-}DI]$ and $k \sim k_{cat}$. By fitting the dehydrogenase activities with the addition of free FMN molecules, we were able to estimate the binding of FMN to DI protein**.** As shown in **Figure 10B,** the apparent dissociation constant ($K_{d,\ app}$) of FMN with DI protein was ~ 0.37 nM, which supported our hypothesis that the tightly bound FMN-DI contributed to the dehydrogenase activity. Similarly, we also titrated the addition of free FMN into a fresh DI solution for enhancing oxidase activity. As shown in **Figure 10C**, the NADH oxidation by FMN-DI protein was increased with the addition of excess FMN from 0 to 128 μM. For control, free FMN by itself only showed weak oxidase activity at high micro-molar concentrations. As described above, the oxidase activity was directly correlated to the concentration of 'FMN-$DI_{(O2)}$ complex' (FMN-$DI_{(O2)}$ has stronger NADH oxidase activity). As shown in **Figure 10D**, the apparent dissociation constant of FMN binding to the DI protein for FMN-$DI_{(O2)}$ was $K_{d,app}$ ~ 146 μM by fitting the oxidase activities with the addition of free FMN molecules. Obviously, the apparent K_d value of FMN-$DI_{(O2)}$ for oxidase activity was much larger than that of FMN-$DI_{(DH)}$ for dehydrogenase activity. This result further supported our hypothesis that the tight FMN-DI interaction contributed to the strong dehydrogenase activity. Conversely, the weak FMN-DI interaction was responsible for the increased oxidase activity due to dissociated $FMNH_2$ reacting with O_2. The addition of excess FMN into an aged FMN-DI solution can also restored its dehydrogenase activity to ~ 50% of a fresh FMN-DI solution.

Wash Steps	Fresh FMN-DI			Old FMN-DI		
	A280	A452	A452/A280	A280	A452	A452/A280
Prior to wash	8.67	1.11	0.13	8.22	1.13	0.14
1	7.99	0.96	0.12	7.41	0.53	0.072
2	7.71	0.93	0.12	6.62	0.32	0.048

Table 1. Removal of FMN from DI protein by molecular-weight cutoff filtration.

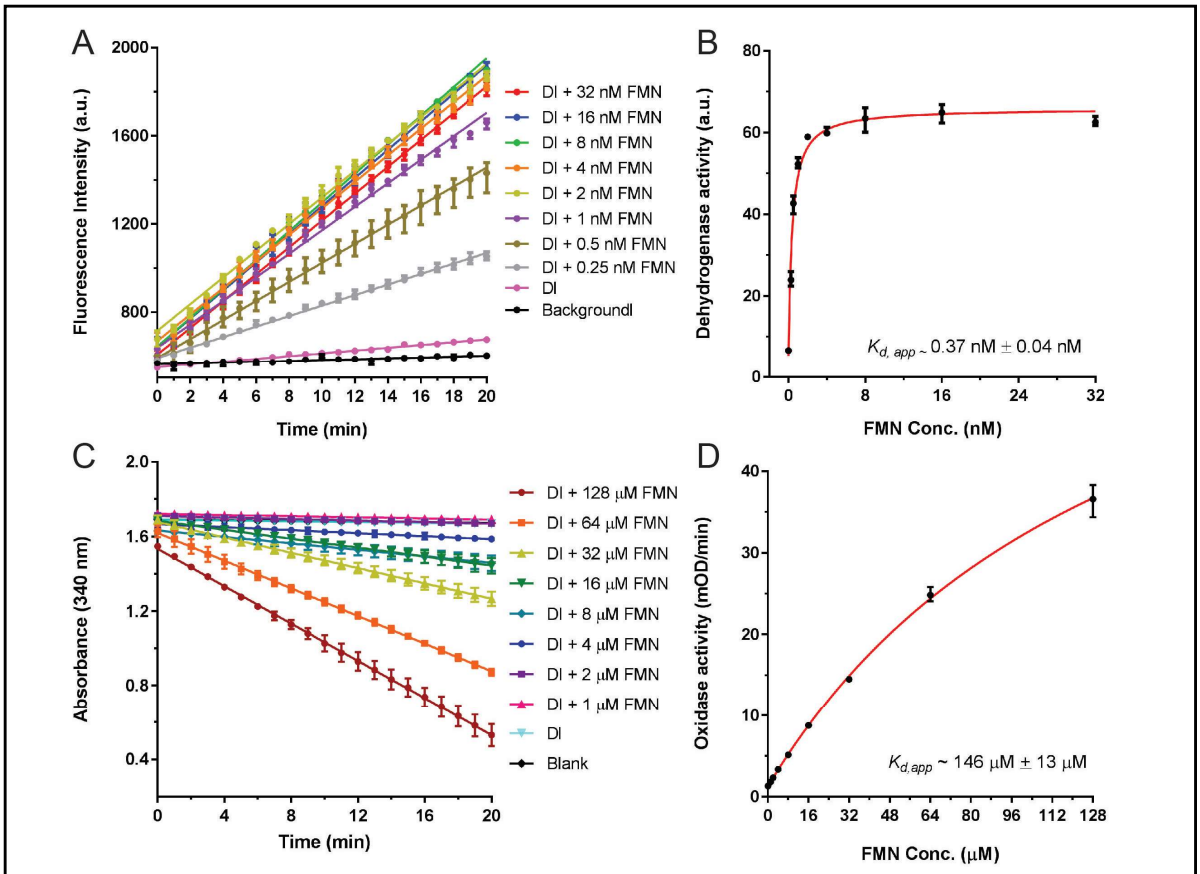

Figure 10. The titration of free FMN molecules for affecting activities of a DI protein solution. (A) Titration of excess FMN molecules into a DI protein solution for enhancing the dehydrogenase activity: 0.5 nM DI protein solution is incubated with 0 – 16 nM free FMN, and is assayed by adding 500 μM NADH and 500 μM resazurin in pH 7.5, 1×TBS buffer. (B) The initial velocities of reactions are fitted with the addition of free FMN molecules for estimating the apparent dissociation constant of FMN binding to DI for dehydrogenase activity. (C) Titration of excess FMN molecules into a DI protein solution for enhancing the oxidase activity: 200 nM DI solution is incubated with 0 – 128 μM free FMN, and is assayed by adding 1000 μM NADH in pH 7.5, 1×TBS buffer. (D) The initial velocities of reactions are fitted with the addition of free FMN molecules for estimating the apparent dissociation constant of FMN binding to DI for oxidase activity.

Circular dichroism (CD) was used to analyze the folding state of FMN-DI complex. As shown in **Figure 11A**, both the fresh FMN-DI and the old FMN-DI solutions showed negative CD signals at 210 -222 nm, which suggested alpha helical structures. The old FMN-DI solution showed a shifted positive peak at ~198 nm as compared with the positive peak at ~ 193 nm for the fresh FMN-DI solution. This shifted absorbance might suggest an increased beta-sheet structure for the old FMN-DI solution. As shown in **Figure 11B**, the binding of FMN to DI was also analyzed by CD, where the fresh FMN-DI solution showed a positive CD signal at ~ 450 nm with the indication of protein-bound FMN. The old FMN-DI solution showed a relatively weaker CD signal, suggesting the destabilized FMN-DI binding. As a control, the free FMN solution did not show an obvious CD signal at ~ 450 nm. We further tested the protein stability against urea and thermal incubation. As shown in **Figure 11C**, the NADH oxidase activity of a fresh FMN-DI solution first slightly increased as the addition of urea, possibly due to the destabilization of FMN-DI binding. In contrast, the oxidase activity of an old FMN-DI solution quickly decreased as the addition of

urea. For both fresh and old FMN-DI solution, the oxidase activity was completely lost when 4 M urea was added. As shown in **Figure 11D**, the dehydrogenase activity of FMN-DI solution decreased as the addition of urea. However, a fresh FMN-DI solution was more resistant to urea denaturation than an old FMN-DI solution. The urea titration also showed that the FMN-DI binding of a fresh protein solution was tighter than that of an aged solution.

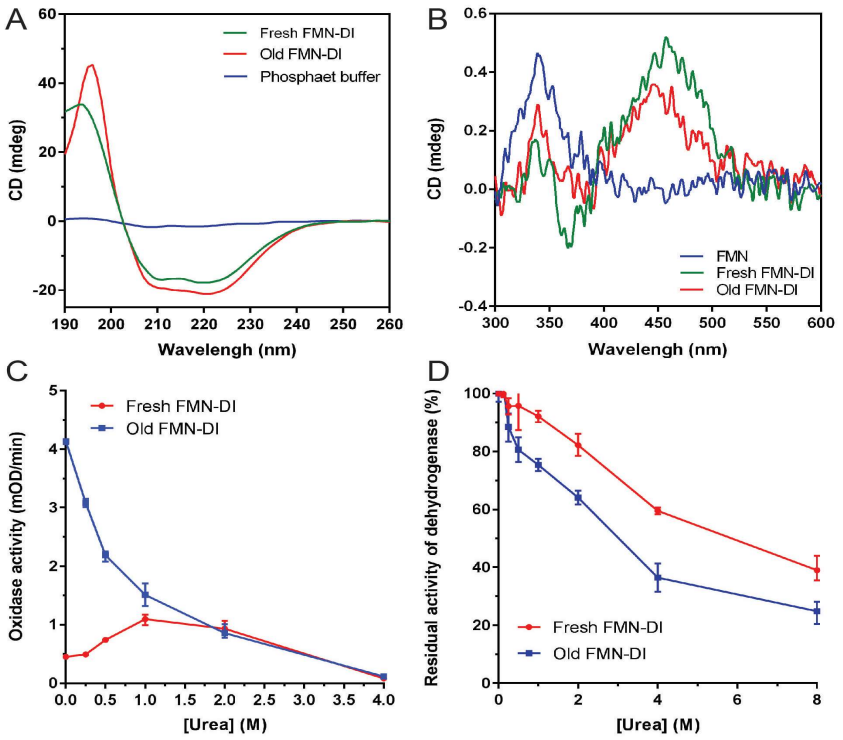

Figure 11. CD spectrum of FMN-DI complexes. (A) CD spectrum of DI proteins from 190 – 260 nm. Condition: 10 μM DI in pH 7.5, 20 mM sodium phosphate buffer. (B) CD spectrum (300 – 600 nm) for 100 μM soutions of free FMN (blue), fresh FMN-DI (green) and old FMN-DI (red). (C) The FMN-DI oxidase activity against the addition of urea. (D) The FMN-DI dehydrogenase activity against the addition of urea.

c. Conclusions and Significance: These results can be applied to the design of a versatile toolbox for modulating enzyme functions, and the development of bio-electroactive, NAD-dependent dehydrogenase pathway for production of biofuels and biochemicals.

III-(3) DNA crowded-enzyme complexes with enhanced activities

As shown in **Figure 12A**, the construction of DNA-crowded enzyme complex involves two steps: (1) the conjugation of an initiator strand to an enzyme (enzyme-I) and (2) the growth of double-strand DNA (dsDNA) on the enzyme surface by the initiator-triggered hybridization chain reaction (HCR). One initiator on the enzyme surface can trigger the growth of a long dsDNA with the alternative hybridization of hairpin 1 and 2. The relative length of dsDNA was determined by the initiator-to-hairpin ratio, where excess hairpins resulted in longer dsDNA by HCR. The long HCR duplex on the enzyme surface behaves as a flexible 'DNA hair' to crowd the enzyme (Non-nick dsDNA's persistence length is ~ 50 nm. But a HCR duplex has many nick points that make it easier to bend). As shown in **Figure 12B**, the gel electrophoresis was used to characterize the growth of dsDNA on the enzyme surface, where larger dsDNA with slower mobility was observed with the addition of more hairpins. The fluorescent imaging of Cy3-labelled enzyme showed that the enzyme was migrated together with the large dsDNA. As shown in **Figure 12C**, dynamic light scattering (DLS) was used to characterize the hydrodynamic diameters of multiple enzyme-HCR

complexes in solution phase. An enzyme-initiator conjugate showed a peak diameter ~ 7 nm. The diameter of enzyme-HCR complexes was increased from ~ 8 nm to ~ 30 nm with the addition of hairpins from 1-fold to 16-fold excess. We also used atomic force microscopy (AFM) to directly visualize DNA-crowded enzymes on mica surface, where long DNA "hairs" were observed with the attachment of bright spots of proteins.

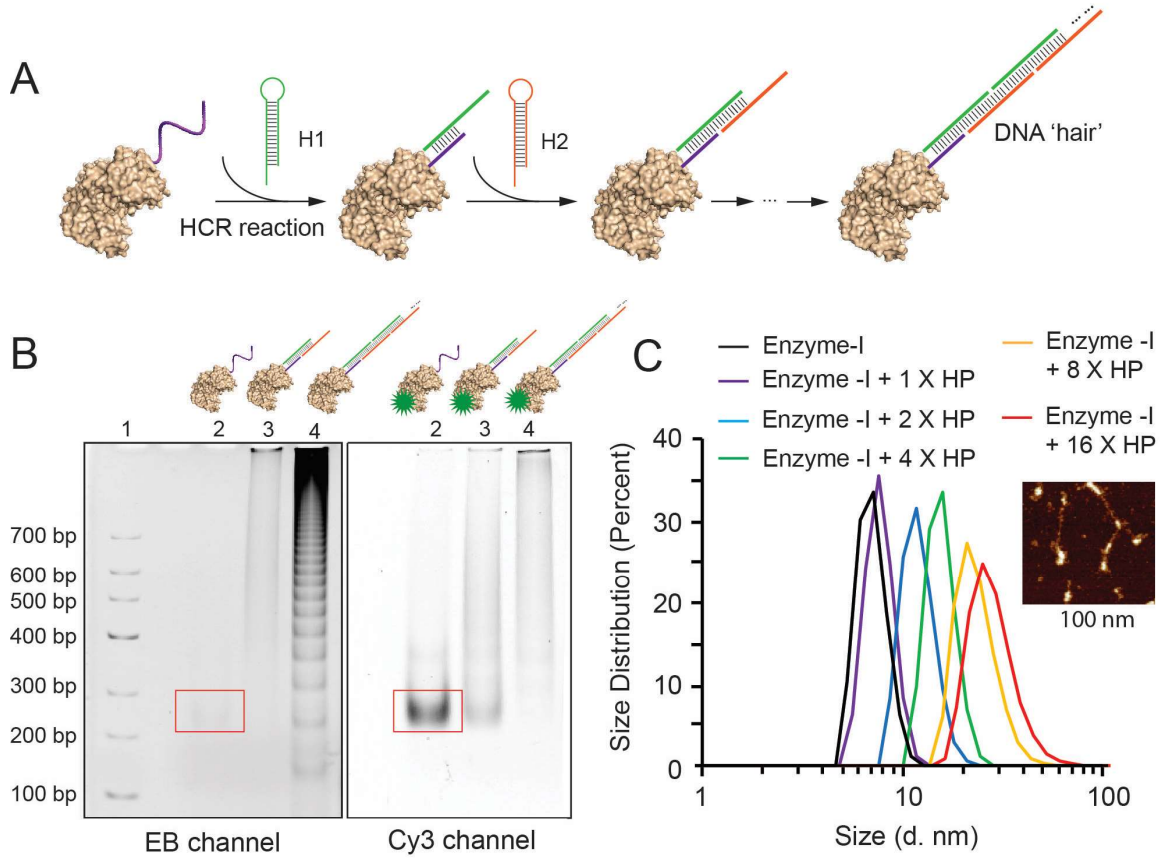

Figure 12. The design and characterization of DNA-crowded enzymes. (A) The construction of long DNA duplex on an enzyme surface by HCR. (B) (3%) PAGE characterization of DNA-crowded enzymes with EB staining (left) of DNA and fluorescent imaging (right) of Cy3-labelled G6PDH. Lane 1: DNA ladder; Lane 2: 1 μM initiator-conjugated G6PDH (G6PDH-I); Lane 3: 1 μM G6PDH-I + hairpins (1×); Lane 4: 1 μM G6PDH-I + hairpins (10 ×). (C) DLS analysis of DNA-crowded enzyme sample with the titration of HPs-to-enzyme ratios. Inset: AFM imaging of DNA-crowded enzyme complex.

Next, we evaluate the enzyme activities depending on the growth of long dsDNA on the enzyme surface. As shown in **Figure 13A**, G6PDH-initiator (G6PDH-I) conjugate was incubated with excess hairpins from 1 to 128-fold for initiating the growth of dsDNA on the enzyme surface by HCR. The activity of G6PDH-I/HCR complex was increased as the addition of more hairpins, with more than 200% enhancement when G6PDH-I was incubated with 16-fold or more hairpins. As a control, non-initiator conjugated enzymes were also incubated with excess hairpins, but these enzymes only showed slightly increased (< 20%) activities. Similar results were also observed for HRP- HRP-HCR complex which showed more than 300% enhanced activity by adding 32-fold or more HPs (**Figure 13B**). These results demonstrated the enzyme activity was significantly boosted

when a long dsDNA was grown on the enzyme surface. To evaluate the effect of labelled numbers for initiator strands, we conjugated and purified HRP with 1, 2 and 3 initiators. Activities of HRP were affected little by conjugating to DNA strands. As shown in **Figure 13C**, HRP-I_2/HCR and HRP-I_3/HCR showed higher activities than HRP-I_1/HCR, possibly due to the fact that more dsDNA duplexes were induced to grow on the enzyme surface. However, many enzymes may show reduced activities as conjugating more DNA molecules (> 3) to the enzyme surface (e.g. G6PDH-I_3) To avoid the significantly damaged activities, we suggested conjugating two initiator strands to one enzyme for triggering dsDNA growth on the enzyme surface.

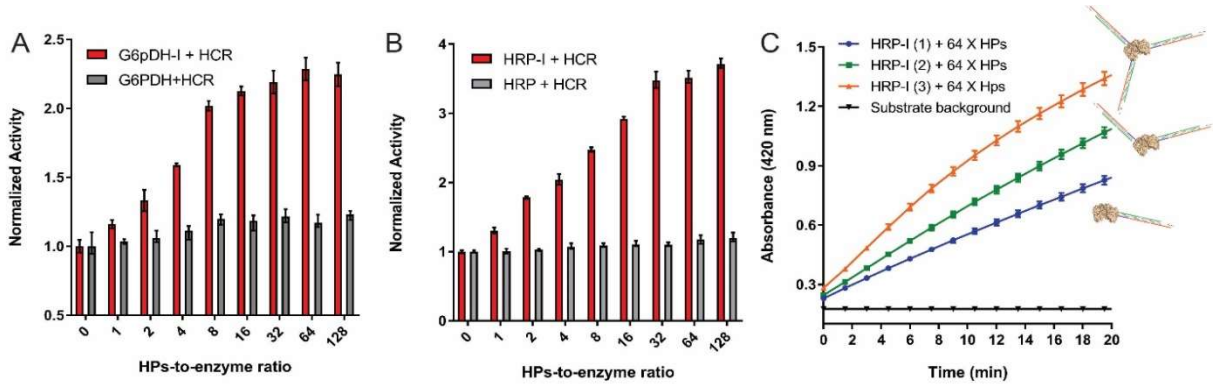

Figure 13. Evaluation of DNA-crowded enzyme complexes. (A) Titration of HPs-to-enzyme ratio for affecting DNA-crowded G6PDH activity; (B) Titration of HPs-to-enzyme ratio for affecting DNA-crowded HRP activity. (C) Titration of labelled initiators per enzyme for affecting DNA-crowded HRP activity. Error bar: range of data.

To gain more mechanistic insight of the enhanced enzyme activities, we tested the Michaelis-Menten kinetics for HRP-I_x/HCR and G6PDH-I_x/HCR complexes. As shown in **Table 2**, HRP-I_1/HCR, HRP-I_2/HCR and HRP-I_3/HCR all showed increased turnover numbers as compared with none-HCR enzymes of HRP-I_1, HRP-I_2, and HRP-I_3, indicating an inherently higher catalytic activity of the enzymes. HRP-I_2/HCR and HRP-I_3/HCR showed ~ 2.7-hold enhancement of k_{cat} values, whereas HRP-I_1/HCR showed less enhancement, ~ 1.6-hold. The difference of enhanced turnover numbers is consistent with the observation that enzymes labelled with more initiator strands produced more activity. Similarly, G6PDH-I_x/HCR complexes also showed higher turnover numbers (~ 2 -3 fold) than non-HCR enzymes. However, G6PDH-I_3/HCR ($k_{cat, NAD}$~ 210 s^{-1}) was less active than G6PDH-I_1/HCR ($k_{cat, NAD}$~ 327 s^{-1}) and G6PDH-I_2/HCR ($k_{cat, NAD}$~ 378 s^{-1}), which could be resulted from the low activity of G6PDH-I_3. In contrast, K_m (Michaelis-Menten constant) values varied little between enzyme-HCR and free enzyme-initiator for most substrates, suggesting that the HCR duplex does not substantially hinder diffusion of small-molecule substrates.

Enzyme	pI	Molecular Weight	Substrate	Enzyme-I		Enzyme-HCR	
				K_m (μM)	k_{cat}(s^{-1})	K_m (μM)	k_{cat}(s^{-1})
HRP-I(1)	8.8	44 kD	H_2O_2	19±2	84±2	19±1	137±2
HRP-I(2)	8.8	44 kD	H_2O_2	21±2	74±1	23±1	203±2
HRP-I(3)	8.8	44 kD	H_2O_2	19±1	77±1	24±1	225±3
G6PDH-I(1)	4.3	100 kD	G6P	335±44	105±5	333±30	289±9
			NAD^+	627±63	129±5	625±35	326±8
G6PDH-I(2)	4.3	100 kD	G6P	446±49	83±3	447±42	285±10
			NAD^+	673±78	133±7	673±68	378±16
G6PDH-I(3)	4.3	100 kD	G6P	602±52	48±2	519±42	144±5
			NAD^+	785±60	61±2	711±51	210±6

Table 2. Enzyme kinetic data (values of K_m and k_{cat}) for each individual enzyme-HCR complex in comparison with the values for enzyme-initiator conjugates. The Michaelis-Menten plots of each enzyme and the conditions of the enzyme activity measurements can be found in the method. The pI values of the enzymes were obtained from brenda-enzymes.org.

In addition to enhanced turnover numbers for catalysis, the enzyme-HCR complex also showed increased stability against various denaturation conditions, such as long-term storage, freeze-thaw cycles and thermal incubation. As shown in **Figure 14A**, we tested the stability of enzyme solutions against long-term storage at room temperature (25 °C). All HRP-HCR complexes showed more stable activities as compared with HRP wildtype. For example, at the 10^{th} week, HRP-HCR complexes retained ~ 50% of original activities, whereas individual HRP only retained ~20% of original activities. In **Figure 14B**, HRP-HCR complexes were more stable against multiple freeze-thaw cycles than wildtype HRP. It was also noticed that HRP-I_3/HCR (retain~ 90% activity at 10^{th} cycle) was more stable than HRP-I_1/HCR (retain~ 63% activity at 10^{th} cycle) and HRP-I_2/HCR (retain~ 75% activity at 10^{th} cycle), as well as HRP wildtype (retain~ 24% activity at 10^{th} cycle). To rule out the potential absorption of enzymes onto the tube walls during the incubation, we used a Cy3-labelled enzyme to monitor the solution fluorescence during the incubation period. The Cy3-labelled enzyme solution did not show significant decrease of fluorescence during either long-term storage or freeze-thaw cycles, which suggested that the concentration of solution enzymes did not alter significantly during the incubation. In **Figure 14C**, HRP-HCR complexes showed an increased thermal stability of enzyme from 45 – 70 °C.

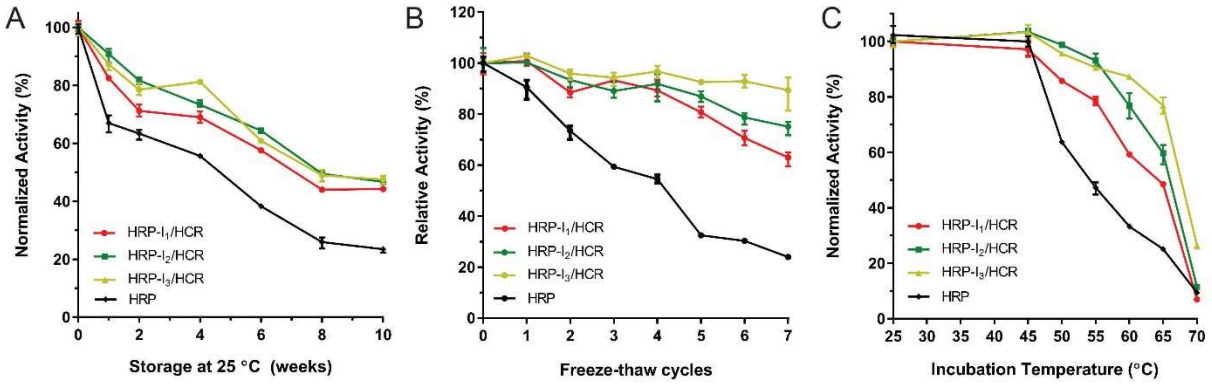

Figure 14. Evaluating the stability of DNA-crowded enzyme against (A) long-term storage under room temperature; (B) freeze-thaw cycles and (C) thermal incubation.

Conclusions and Significance: In summary, we have developed a simple and robust method for assembling DNA-crowded enzyme complex with promoted enzyme activity and increased stability. By conjugating an initiator strand to an enzyme, we were able to initiate the growth of long dsDNA on the enzyme surface to increase local DNA crowding. The number and length of DNA duplexes were controlled by the copies of labelled DNA initiators and the addition of hairpins. The enzyme-HCR complexes exhibited increased turnover numbers of 2- to 3-fold higher than that of the free enzymes. Conversely, the K_m values remain similar between enzyme-HCR complexes and free enzymes, indicating an uninterrupted diffusion of small-molecule substrates and products through the surface-grown DNA duplexes. The enhanced activities of enzyme-HCR complexes were consistent with recently reported enzyme/DNA hybrid nanostructures, which might be attributed to the local DNA crowding with high density of negatively charged phosphate groups. This effect appears consistent with recent independent evidence that many conserved metabolic enzymes are stabilized by polyphosphate and associate non-specifically with nucleic acids through cryptic binding sites, thus taking advantage of the high polyanionic DNA and RNA contents of the cell. Unlike DNA origami nanocages with application limit of low achievable concentration, the small production scale and the high cost of complex oligonucleotides, the assembly of DNA-crowded enzyme particles only involved three strands of one initiator and two hairpin substrates. The concentration and production of enzyme particles can be easily scaled up to high micro-molar concentrations for practical use. In the future, it may be feasible to crosslink multiple DNA-crowded enzyme particles into nanocrystals and hydrogels which can stabilize enzymes against various denaturations, as well as facilitating the multi-enzyme catalysis. The DNA-crowded enzyme particles may also find utility in theranostic applications as therapeutic agents and drug delivery.

IV. Future Directions:

a. DNA-mediated assembly hairpin for engineering enzyme functions. We will use DNA-mediated proximity assembly circuits (Developed from YIP project) to regulate the spatial interaction of an enzyme and a cofactor for activating or inhibiting a pathway reaction. The proximity assembly of an enzyme/cofactor pair will be regulated by the external input molecules and substrates or products of the reaction pathway, which provides another mechanism of engineering feedback function of a biochemical pathway.

b. ***DNA-crowded enzyme complexes.*** We will perform mechanistic studies of DNA-crowded enzyme complex and understand how DNA crowded nanostructures modify the local nanoenvironment. For example, we will investigate hydration layer on the surface or within DNA nanostructures and probe the local pH values that are modified by DNA nanostructures.

V. Publications and presentations from this reporting period:

V.1. Total number of papers published in peer reviewed journals: 11

1. Sung Won Oh, Adriana Pereira, Ting Zhang and **Jinglin Fu*** "DNA-Regulated Proximity Assembly Circuit for Actuating Biochemical Reactions", Angewandte Chemie **2018**, 57, 13086-13090. doi: 10.1002/anie.201806749.
2. Yuhe R. Yang, **Jinglin Fu**, Shaun Wootten, Xiaodong Qi, Minghui Liu, Hao Yan and Yan Liu* "2D Enzyme Cascade Network with Efficient Substrate Channeling by Swinging Arms", ChemBioChem **2018**, 19, 212-216.
3. Scott Huston, John Collins, Fangfang Sun, Ting Zhang, Timothy D. Vaden, Y. –H. Percival Zhang and **Jinglin Fu*** "An Activity Transition from NADH Dehydrogenase to NADH Oxidase during Protein Denaturation", BioTechnology and Applied Biochemistry **2018**, 65, 286-293.
4. John Collins, Ting Zhang, Sung Won Oh, Robert Maloney and **Jinglin Fu*** "DNA-Crowded Enzyme Nanoparticles with Enhanced Activities and Stabilities", Chem Comm. 2017, 53, 13059–13062
5. **Jinglin Fu***, Gabriele Stankeviciute, Sung Won Oh, John Collins Yinghui Zhong and Ting Zhang "Self-assembled Nucleic Acid Nanostructures for Cancer Theranostics Medicines", Current Topics in Medicinal Chemistry **2017**, 17, 1-14.
6. **Jinglin Fu***, Renee Yang, Soma Dhakal, Zhao Zhao, Minghui Liu, Ting Zhang, Nils Walter and Hao Yan "Assembly of Multi-Enzyme Complexes on DNA Nanostructures" Nature Protocols **2016**, 11, 2243–2273.
7. Minghui Liu, Jinglin Fu, Xiaodong Qi, Shaun Wootten, Neal W. Woodbury, Yan Liu and Hao Yan* "A three-enzyme pathway with an optimized geometric arrangement to facilitate substrate transfer" ChemBioChem 2016, 17, 1097-1101.
8. John Collins, Ting Zhang, Scott Huston, Fangfang Sun, Percival Zhang and **Jinglin Fu*** "A Hidden Transhydrogen Activity of A FMN-Bound Diaphorase under Anaerobic Conditions" PLoS One**2016,** DOI: 10.1371/journal.pone.0154865.
9. Zhao Zhao+, **Jinglin Fu***+, Soma Dhakal, Alexander Johnson-Buck, Minghui Liu, Ting Zhang, Neal Woodbury, Yan Liu, Nils G. Walter* and Hao Yan* "Nano-caged Enzymes with Enhanced Activity and Increased Stability against Protease Digestion" Nature Communications 2016, 7, 10619.
10. Ting Zhang, John Collins, Georgia A. Arbuckle-Keil and **Jinglin Fu*** "DNA-directed Assembly of Conductive Nanomaterials" Advanced Science, Engineering and Medicine 2015, 7, 1019-1032.
11. Ting Zhang, John Collins, **Jinglin Fu*** "Single-Molecule Sensing of Biomolecular Interactions on DNA Nanostructures" Current Nanoscience 2015,11, 727-735.

V.2. Total number of books: 1

Jinglin Fu* and Tianran Li "Spatial Organization of Enzyme Cascade on a DNA Origami Nanostructure", invited book chapter for "3D Nucleic Acid Nanostructures — Methods and Protocols", *Methods in Molecular Biology*, **2016**, Humana Press.

V.3. Total number of papers published in non-peer-reviewed journals: 1

Jinglin Fu,* Bryce Sadtler, Ian Wheeldon and Zhuangqun Huang "A Special Issue on How Can We Learn from Biology to Create New Functional Materials?" *Advanced Science, Engineering and Medicine* **2015**, 7, 1007-1008.

V.4. Total numbers of manuscript under consideration in journals: 2

1. Ting Zhang, Jia Nong, Nouf Alzahrani, Zhicheng Wang, Tristan Meier, Dong Gyu Yang, Yonggang Ke, Yinghui Zhong and **Jinglin Fu*** "Self-assembly of DNA-Minocycline Complexes by Metal Ions with Controlled Drug Release" *ACS Applied Materials & Interfaces*, under peer review.

2. **Jinglin Fu***, Sung Won Oh, Kristin Monckton, Georgia Arbuckle-Keil, Yonggang Ke and Ting Zhang "Bio-mimetic Compartments Scaffolded by Nucleic Acid Nanostructures" *Small*, under peer review.

V.5. Total number of presentations (Presented by Dr. Fu): 20

1. "DNA-Regulated Proximity Assembly Circuit for Actuating Biochemical Reactions", invited talk, the 7th International Conference on DNA Nanotechnology, Chongqing, China, **June 2018**.
2. "Logic-gated Proximity Assembly of Biochemical Reactions for Sensing Targets", invited talk, Thermal Analysis Forum Delaware Valley (TAFDV), Rutgers University-Camden, **2018**.
3. "DNA-scaffolded Proximity Assembly of Biochemical Reactions" invited talk, Department of Chemistry at Rowan University, **2018**.
4. "DNA-based Proximity Assembly Circuit for Actuating Biochemical Reactions", invited talk, CCIB retreat, Rutgers University-Camden, **2017**.
5. "DNA-nanocaged enzyme complex with controlled spatial confinements", invited talk, New York Nanoscience Discussion Group at New York University, **2017**.
6. "DNA-crowded enzyme nanoparticles with improved activity and stability", oral presentation, the 6th International Conference on DNA Nanotechnology **2017**, Beijing, China
7. "Assembly of Bio-mimetic Multienzyme Complex on DNA Nanoscaffolds", oral presentation, 254th ACS National Meeting **2017**, Washington DC.
8. "Develop DNA-crowded enzyme nanoparticles for promoting activity and stability", oral presentation, ACS Middle Atlantic Regional Meeting **2017**, Hershey.
9. "Spatially Interactive Biomolecular Networks Organized by Nucleic Acids Nanostructures", invited talk, East Lake International Forum for Outstanding Overseas Young Scholars **2016**, Wuhan, China.
10. "DNA-crowded enzyme complexes with improved activity and stability", oral presentation, 252nd ACS National Meeting **2016**, Philadelphia.
11. "Assembly of multi-enzyme complexes on DNA nanoscaffolds", oral presentation, 252nd ACS National Meeting **2016**, Philadelphia.
12. "Spatially Interactive Biomolecular Networks Organized by DNA Architectures", invited talk, National Center for Nanoscience and Technology at Beijing, China, May 20, **2016**.
13. "Spatially interactive biomolecular networks", invited talk, Meeting with New Jersey Health Foundation, Rutgers University-Camden, **2015**.
14. Spatially Interactive Biomolecular Networks Organized by DNA Architectures", invited talk, College of Electronic Science & Engineering, Jilin University, Changchun, China, Oct. 28th, **2015**. (Invited by Prof. Haiyu Wang at Jilin University)
15. "Spatially Interactive Biomolecular Networks Organized by DNA Architectures", invited talk, 3rd Young Chemists Forum, Zhejiang University, Hangzhou, China. Oct. 30 – Nov. 1, **2015**
16. "Biomimetic catalytic complexes organized by DNA nanoscaffolds ", oral presentation, 250th ACS National Meeting **2015**, Boston.
17. "Biomimetic Catalytic Complexes Organized by DNA Nanoscaffolds", oral presentation, ACS Northeast Regional Meeting **2015**, Ithaca, NY. (Presented by Jinglin Fu)

18. "Structural DNA Nanotechnology in Molecular Biomimetics", invited talk, Rowan University, **2015**. (Presented by Jinglin Fu)
19. "Spatially-Organized Multi-Enzyme Systems", invited talk, Ultrafast Optical Processes Laboratory at University of Pennsylvania, **2015**. (Presented by Jinglin Fu)
20. "BioInspired Molecular Complex on DNA nanoscaffods", invited talk, South Jersey ACS meeting, **2014**. (Presented by Jinglin Fu)

VI. Honors and awards:

- Certificate of a mentorship, Army Education Outreach Program (AEOP), **2018**
- Cottrell College Science Award, **2015**
- Certificate of a Research Mentorship, Rutgers-Camden, **2015-2018**
- Proclamation, Board of Chosen Freeholders of the County of the Camden, **2015**
- Army Research Office Young Investigator award, **2014**

VII. Patents disclosed during the reporting period: 2

1. **Jinglin Fu**, Sung Won Oh and Adriana Pereira "DNA Logic-gated Proximity Assembly Circuit for Biochemical Sensing" U.S. Patent Application No. 62/647,014.
2. **Jinglin Fu**, John Collins and Ting Zhang "DNA-crowded Enzyme Complex with Controlled Spatial Confinements" US Provisional Patent. App. No. 62/482,882.

VIII. Students Training

1. Total number of undergraduate bachelor degrees awarded: 8

Adriana Pereira, Brett Vaccaro, Gina Disalvo, Gabriele Stankeviciute, Scott Huston, Robert Maloney, John Collins, Sung Won Oh

2. Total number of Master's degree awarded: 3

John Collins, Nouf Alzhrani, Samirah Ghalib

3. Other graduate students: 2

Ariel Lane, Tianran Li

4. Total number of high school students sponsored for summer research: 5

Chae Lee, Olivia Zapfe, Tristan Meier, Elizabeth Bolarinwa, Grace Kresge

5. Total Number of NSF REU students: 2

Karen Gu, Angela Sun

IX Dissemination

1. 6/27/2018: Rutgers University–Camden Professor Gives South Jersey High School Students Research Experience through the Army Educational Outreach Program https://news.camden.rutgers.edu/2018/06/rutgers-university-camden-professor-gives-south-jersey-high-school-students-research-experience-through-the-army-educational-outreach-program/

2. 7/26/2017: Army Education Outreach Program Provides Research Experience in Labs for Undergraduates and High School Students.
https://news.camden.rutgers.edu/2017/07/army-education-outreach-program-provides-research-experience-in-labs-for-undergraduates-and-high-school-students/
3. 7/23/2015: Army Education Outreach Program Supports Two Summer Research Projects
https://news.camden.rutgers.edu/2015/07/army-education-outreach-program-supports-two-summer-research-projects/
4. 2/22/2015: Army Education Outreach Program Supports Research Projects for High School and Undergraduate Students at Rutgers University–Camden
https://news.rutgers.edu/news/army-education-outreach-program-supports-research-projects-high-school-and-undergraduate-students/20150211#.XFn9glxKhPZ